



MÔNICA SIQUEIRA FERREIRA

**“ESTUDOS LIPIDÔMICOS APLICADOS À  
ESQUISTOSSOMOSE”**

CAMPINAS

2014



**UNIVERSIDADE ESTADUAL DE CAMPINAS  
FACULDADE DE CIÊNCIAS MÉDICAS**

**MÔNICA SIQUEIRA FERREIRA**

**“ESTUDOS LIPIDÔMICOS APLICADOS À  
ESQUISTOSSOMOSE”**

**Orientador: Prof. Dr. Rodrigo Ramos Catharino**

Tese de Doutorado apresentada ao Programa de Pós Graduação em Fisiopatologia Médica da Faculdade de Ciências Médicas da Universidade Estadual de Campinas para obtenção do título de Doutora em Ciências.

**ESTE EXEMPLAR CORRESPONDE À VERSÃO FINAL DA TESE  
DEFENDIDA PELA ALUNA MÔNICA SIQUEIRA FERREIRA E  
ORIENTADA PELO PROF. DR. RODRIGO RAMOS CATHARINO**

Assinatura do Orientador

---

**CAMPINAS**

**2014**

Ficha catalográfica  
Universidade Estadual de Campinas  
Biblioteca da Faculdade de Ciências Médicas  
Maristella Soares dos Santos - CRB 8/8402

F413e

Ferreira, Mônica Siqueira, 1986-  
Estudos lipidômicos aplicados à esquistossomose /  
Mônica Siqueira Ferreira. -- Campinas, SP : [s.n.], 2014.

Orientador : Rodrigo Ramos Catharino.  
Tese (Doutorado) - Universidade Estadual de  
Campinas, Faculdade de Ciências Médicas.

1. Parasitologia. 2. Espectrometria de massas. 3.  
Lipídeos. 4. *Schistosoma mansoni*. I. Catharino, Rodrigo  
Ramos, 1977-. II. Universidade Estadual de Campinas.  
Faculdade de Ciências Médicas. III. Título.

Informações para Biblioteca Digital

**Título em outro idioma:** Lipidomic studies applied to schistosomiasis

**Palavras-chave em inglês:**

Parasitology

Mass spectrometry

Lipids

*Schistosoma mansoni*

**Área de concentração:** Fisiopatologia Médica

**Titulação:** Doutora em Ciências

**Banca examinadora:**

Rodrigo Ramos Catharino [Orientador]

Gisele Leticia Alves

Daisy Machado

Rodinei Augusti

Luciana Maria de Hollanda

**Data de defesa:** 29-08-2014

**Programa de Pós-Graduação:** Fisiopatologia Médica

## BANCA EXAMINADORA DA DEFESA DE DOUTORADO

MONICA SIQUEIRA FERREIRA

Orientador (a) PROF(A). DR(A). RODRIGO RAMOS CATHARINO

### MEMBROS:

1. PROF(A). DR(A). RODRIGO RAMOS CATHARINO Rodrigo Ramos Catharino

2. PROF(A). DR(A). RODINEI AUGUSTI Rodinei Augusti

3. PROF(A). DR(A). GISELE LETICIA ALVES Gisele Letícia

4. PROF(A).DR(A). LUCIANA MARIA DE HOLLANDA Luciana Maria de Hollanda

5. PROF(A).DR(A). DAISY MACHADO Daisy Machado

Programa de Pós-Graduação em Fisiopatologia Médica da Faculdade de Ciências Médicas da Universidade Estadual de Campinas

Data: 29 de agosto de 2014

## RESUMO

Com a grande incidência de resistência ao único fármaco utilizado no tratamento de esquistossomose, Praziquantel (PZQ), e relatos de diferentes níveis de virulência do parasita, o controle da doença tem se tornado cada vez mais difícil. Além disso, o método de diagnóstico convencional demanda tempo e grande preparo amostral. Num cenário clínico, quanto mais rápido o diagnóstico, maiores as chances de sucesso no tratamento da doença. Tendo em vista esse escopo, apresentamos uma nova plataforma “ômica” – a Parasitômica, que propõe o uso de metodologias simplificadas e de grande eficácia em termos de preparo de amostra e facilidade na aquisição de dados voltados a área de parasitologia, englobando diagnóstico, tratamento e elucidação de vias e mecanismos de ação. Amostras de diferentes cepas de *Schistosoma mansoni*, bem como diferentes estágios e tratamento com PZQ, foram analisadas através da técnica de espectrometria de massas por imagem (MALDI-MSI) e por alta resolução (ESI-HR-FTMS), pela integração de dados tanto analíticos quanto estatísticos. É possível a caracterização e diferenciação química de cada sexo e cepa do *S. mansoni*, bem como a visualização das alterações na composição molecular de vermes submetidos ao tratamento com PZQ. Tais resultados poderão ser úteis como potenciais alvos de novos fármacos. Nossos resultados também demonstram uma possível forma de futuro diagnóstico da esquistossomose pela análise da urina utilizando a parasitômica.

## ABSTRACT

With the large incidence of resistance to the only drug used to schistosomiasis treatment, Praziquantel (PZQ), and reports of different levels of parasite virulence, disease control has become increasingly difficult. Furthermore, the conventional diagnosis method is time consuming and requires extensive sample preparation. In a clinical setting, the sooner the diagnosis is, the greater are the chances of successful disease treatment. Within this scope, we present a new “omic” platform – Parasitomics, which proposes the use of simple and effective methods in terms of sample preparation and readiness of data acquisition focused on parasitology, including diagnosis, treatment and elucidation of pathways and mechanisms of action. Samples with different strains of *Schistosoma mansoni*, as well as different stages of life cycle and treatment with PZQ, were analyzed by mass spectrometry imaging (MALDI-MSI) and by high-resolution technology (ESI-HR-FTMS), through the integration of analytical and statistical data. Results have enabled the characterization and chemical differentiation of each sex and strain of *S. mansoni*, as well as the visualization of molecular composition changes in worms’ body submitted to PZQ treatment. These results could be helpful on unraveling potential targets for new drugs. Our results also demonstrated a possible form of future schistosomiasis diagnosis by urine analysis using the parasitomics platform.

## SUMÁRIO

<b>RESUMO.....</b>	<b>ví</b>
<b>ABSTRACT.....</b>	<b>vii</b>
<b>DEDICATÓRIA.....</b>	<b>ix</b>
<b>AGRADECIMENTOS.....</b>	<b>x</b>
<b>INTRODUÇÃO GERAL.....</b>	<b>17</b>
<b>REFERÊNCIAS DA INTRODUÇÃO.....</b>	<b>30</b>
<b>OBJETIVOS.....</b>	<b>33</b>
<b>CAPÍTULO 1 – ESPECTROMETRIA DE MASSAS POR IMAGEM: UMA NOVA VISÃO NA DIFERENCIACÃO DE CEPAS DE <i>SCHISTOSOMA MANSONI</i>.....</b>	<b>34</b>
Abstract.....	35
Introdução.....	36
Materiais e Métodos.....	38
Resultados.....	41
Discussão.....	47
Conclusão.....	50
Referências.....	52
<b>CAPÍTULO 2 – REVELANDO ALVOS MOLECULARES DE PRAZIQUANTEL UTILIZANDO ESPECTROMETRIA DE MASSAS POR IMAGEM: UMA ABORDAGEM RÁPIDA APLICADA PARA <i>SCHISTOSOMA MANSONI</i>.....</b>	<b>54</b>
Abstract.....	55
Introdução.....	56
Materiais e Métodos.....	58
Resultados.....	60
Discussão.....	68
Referências.....	73
<b>CAPÍTULO 3 – ANALISANDO O CICLO DE VIDA DO <i>SCHISTOSOMA MANSONI</i> UTILIZANDO ESPECTROMETRIA DE MASSAS DE ALTA-RESOLUÇÃO.....</b>	<b>77</b>
Abstract.....	78
Introdução.....	80
Materiais e Métodos.....	83
Resultados.....	86
Discussão.....	94
Conclusão.....	97
Referências.....	98
<b>CONCLUSÃO GERAL.....</b>	<b>100</b>
<b>PERSPECTIVAS FUTURAS.....</b>	<b>102</b>

## **DEDICATÓRIA**

Dedico este trabalho à minha família e ao meu marido, que sempre me apoiaram em todas as decisões e nunca mediram esforços pra me ajudar a chegar até aqui. Amo vocês!

## **AGRADECIMENTOS**

Agradeço ao **Professor Rodrigo Catharino** (Doctor Rods!), por ter acreditado em mim e me dado a oportunidade de crescer! Obrigada pela confiança, por todo o aprendizado, paciência e, principalmente, pela amizade!

**Mãe, pai, Juninho e Valesca**, obrigada pelo apoio, pelos esforços e pela paciência nos tempos difíceis. Apesar da distância, estão sempre presentes e isso faz toda a diferença!

**Dani**, meu lindo, meu companheiro de todas as horas. Não sei como seria sem a sua ajuda! Obrigada por tudo! Amo você!

Aos meus amigos/família Innovare: **Dioki, Cibs, Tatimel, João, Jenny, Gus, Maico, Lívia e Nats**, obrigada por me ajudarem! Nossa união e descontração durante cada projeto são os maiores diferenciais! E não importa o caminho que cada um seguirá. Farei questão de manter contato e reunir sempre que possível! Afinal, esse é o laboratório mais divertido do mundo!

**Sil**, minha amiga, dedico esse trabalho também a você! Obrigada pela amizade e confiança. Você é um exemplo, como pessoa e como profissional, e eu te admiro muito!

Aos demais amigos que também participaram dessa jornada, muito obrigada! Impossível citar todos e suas respectivas participações, mas deixo aqui minha gratidão!

**Obrigada, galera!**

**Mônica Siqueira Ferreira**

## LISTA DE ABREVIATURAS

<b>9-AA</b>	9-aminoacridina
<b>AChE</b>	Acetylcholinesterase
<b>BH</b>	Cepa de <i>Schistosoma mansoni</i> proveniente de Belo Horizonte
<b>Cer</b>	Ceramida
<b>CHCA</b>	Ácido alfa-ciano hidróxicinâmico
<b>CID</b>	<i>Collision-induced dissociation</i>
<b>DA</b>	Ácido dodecanóico ( <i>Dodecanoic acid</i> )
<b>DAG ou DG</b>	Diacilglicerol
<b>DESI</b>	<i>Desorption electrospray ionization</i>
<b>DHB</b>	2,5-diidroxibenzóico
<b>ESI</b>	<i>Electrospray ionization</i>
<b>FBH</b>	Vermes adultos fêmeas da cepa de Belo Horizonte
<b>FCT</b>	Vermes adultos fêmeas controle
<b>FPZQ</b>	Vermes adultos fêmeas submetidos a tratamento com praziquantel
<b>FSE</b>	Vermes adultos fêmeas da cepa de Sergipe
<b>FT-ICR</b>	<i>Fourier transform íon cyclotron resonance</i>
<b>Gal-Cer</b>	Galactosilceramida ( <i>Galactosylceramide</i> )
<b>GC</b>	Cromatografia gasosa ( <i>Gas chromatography</i> )
<b>GLC</b>	Glicosilceramida ( <i>Glucosylceramide</i> )
<b>GSL</b>	Glicoesfingolípideo ( <i>Glycosphingolipid</i> )
<b>HPLC</b>	<i>High performance liquid chromatography</i>
<b>HR-FTMS</b>	<i>High-resolution Fourier transform mass spectrometry</i>

<b>IFN-γ</b>	Interferon gama
<b>LAESI</b>	<i>Laser ablation electrospray ionization</i>
<b>LC</b>	Cromatografia líquida ( <i>Liquid chromatography</i> )
<b>LPG</b>	Lisofosfogliceróis ( <i>Lysophosphoglycerols</i> )
<b>MALDI</b>	<i>Matrix-assisted laser desorption/ionization</i>
<b>MBH</b>	Vermes adultos machos da cepa de Belo Horizonte
<b>MCT</b>	Vermes adultos machos controle
<b>MPZQ</b>	Vermes adultos machos submetidos a tratamento com praziquantel
<b>MS</b>	Espectrometria de massas ( <i>Mass spectrometry</i> )
<b>MSE</b>	Vermes adultos machos da cepa de Sergipe
<b>MSI</b>	Espectrometria de massas por imagem ( <i>Mass spectrometry imaging</i> )
<b>MS/MS</b>	Espectrometria de massas em <i>tandem</i>
<b>OSM</b>	Organização de Saúde Mundial
<b>PA</b>	Ácido fosfatídico ( <i>Phosphatidic Acid</i> )
<b>PBS</b>	Tampão fosfato-salina ( <i>Phosphate buffered saline</i> )
<b>PC</b>	Fosfatidilcolina ( <i>Phosphatidylcholine</i> )
<b>PCA</b>	Análise de componentes principais ( <i>Principal component analysis</i> )
<b>PE</b>	Fosfoetanolamina ( <i>Phosphoethanolamine</i> )
<b>PG</b>	Fosfoglicerol ( <i>Phosphoglycerols</i> )
<b>PI</b>	Fosfoinositol ( <i>Phosphoinositol</i> )
<b>PKC</b>	Proteína quinase C
<b>PL</b>	Fosfolipídeo ( <i>Phospholipid</i> )
<b>PS</b>	Fosfatidilserina ( <i>Phosphatidylserine</i> )
<b>PZQ</b>	Praziquantel
<b>RPMI</b>	Meios <i>Roswell Park Memorial Institute</i>

<b>SE</b>	Cepa de <i>Schistosoma mansoni</i> proveniente de Sergipe
<b>SIMS</b>	<i>Secondary ion mass spectrometry</i>
<b>SJ</b>	Cepa de <i>Schistosoma mansoni</i> proveniente de São José dos Campos - SP
<b>SP</b>	Esfingolipídeos ( <i>sphingolipids</i> )
<b>SR</b>	Cepa de <i>Schistosoma mansoni</i> proveniente do bairro Santa Rosa, Campinas - SP
<b>TAG ou</b>	
<b>TG</b>	Triacilglicerol
<b>TLC</b>	Cromatografia por camada delgada ( <i>Thin-layer chromatography</i> )
<b>TNF-α</b>	Fator de necrose tumoral alfa

## LISTA DE FIGURAS

- Figura 1** Incidência de laser sobre amostra recoberta com matriz. Varredura da amostra pelo laser gera espectros em tempo real e imagem química.....26
- Figura 2** Representative fingerprinting images and spectra of *Schistosoma mansoni* adult worms. The imaging represents a sum of all ions within mass range m/z 600–2000. (A) Male BH strain (MBH); (B) male SE strain (MSE); (C) female BH strain (FBH) and (D) female SE strain (FSE). Positive ion mode.....42
- Figura 3** Representative fingerprinting of *Schistosoma mansoni* adult couple worms. The imaging represents a sum of all ions within mass range m/z 600–2000. (A) Picture of worms analyzed. Gynaecophoric channel in male's body (clear) holding female's body (dark). (B) Worms image generated by MALDI-MSI instrument. Illustrative picture of fingerprinting analysis. (C) Representative fingerprinting (total ion current) spectra. Positive ion mode.....43
- Figura 4** Principal component analysis of *Schistosoma mansoni* adult worms. Ion chemical markers of each group separated by principal component analysis (n = 10/group). The explained variances (X-expl) are shown on inferior part of the figure. ■, male BH strain (MBH); ●, female BH strain (FBH); ♦, male SE strain (MSE) and ▲, female SE strain (FSE).....44
- Figura 5** Adult worm images generated by MS, selected using each of the parent ions in MS/MS mode. Images were acquired as one run for each m/z. Female and male BH strain (FBH and MBH, respectively). Pos, posterior portion; Ant, anterior portion; R, reproductive system; D, digestive system; VS, ventral sucker; OS, oral sucker and GC, Gynaecophoric channel.....46
- Figura 6** Adult worm images generated by MS, selected using each of the parent ions in MS/MS mode. Images were acquired as one run for each m/z. Female and male SE strain (FSE and MSE, respectively). Pos, posterior portion; Ant, anterior portion; R, reproductive system; VS, ventral sucker and OS, oral sucker.....47
- Figura 7** Representative fingerprinting spectra of *S. mansoni* adult worms. (A) Female control (FCT). (B) Male control (MCT). (C) Female treated with PZQ (FPZQ). (D) Male treated with PZQ (MPZQ). Positive ion mode.....62
- Figura 8** Principal Component Analysis (PCA) of *S. mansoni* adult worms. Ion biomarkers of each group separated by PCA (n=5/group). The explained variances (X-expl) are shown on inferior part of the figure. ▲, male negative control (MCT). ●, female negative control (FCT). ♦, male treated with PZQ (MPZQ). ■, female treated with PZQ (FPZQ).....63

<b>Figura 9</b>	Male control adult worm images generated by MS/MS. Pos, Posterior portion. Ant, Anterior portion. T, Tegument. OS, Oral sucker. G, Gut.....	65
<b>Figura 10</b>	Female control adult worm images generated by MS/MS. Pos, Posterior portion. Ant, Anterior portion. R, Reproductive system. G, Gut. T, Tegument.....	66
<b>Figura 11</b>	Male adult worm treated with PZQ images generated by MS/MS. Pos, Posterior portion. Ant, Anterior portion. R, Reproductive system. OS, Oral sucker. G, Gut.....	67
<b>Figura 12</b>	Female adult worm treated with PZQ images generated by MS/MS. Pos, Posterior portion. Ant, Anterior portion. R, Reproductive system. T, Tegument. G, Gut. OS, Oral sucker. VS, Ventral sucker.....	68
<b>Figura 13</b>	Representative fingerprinting spectra and PCA of <i>S. mansoni</i> eggs. Both spectra were acquired in positive ion mode by HR-FTMS. (A) Spectrum of eggs SE strain. (B) Spectrum of eggs BH strain. (C) PCA loadings, demonstrating the two distinct groups (n=5/group). The explained variances (X-expl) are shown on inferior part of the figure. ■, eggs SE strain. ●, eggs BH strain.....	88
<b>Figura 14</b>	Representative fingerprinting spectra and PCA of <i>S. mansoni</i> miracidia. Both spectra were acquired in positive ion mode by HR-FTMS. (A) Spectrum of miracidia SE strain. (B) Spectrum of miracidia BH strain. (C) PCA loadings, demonstrating the two distinct groups (n=5/group). The explained variances (X-expl) are shown on inferior part of the figure. ■, miracidia SE strain. ●, miracidia BH strain.....	89
<b>Figura 15</b>	Representative fingerprinting spectra and PCA of <i>S. mansoni</i> cercariae. Both spectra were acquired in positive ion mode by HR-FTMS. (A) Spectrum of cercariae SE strain. (B) Spectrum of cercariae BH strain. (C) PCA loadings, demonstrating the two distinct groups (n=5/group). The explained variances (X-expl) are shown on inferior part of the figure. ■, cercariae SE strain. ●, cercariae BH strain.....	90
<b>Figura 16</b>	Representative fingerprinting spectra and PCA of urine of mice infected or not by <i>S. mansoni</i> . All spectra were acquired in positive ion mode by HR-FTMS. (A) Spectrum of urine of mice infected by SE strain. (B) Spectrum of urine of mice infected by BH strain. (C) Spectrum of urine of control mice. (D) PCA loadings, demonstrating the three distinct groups (n=15/group). The explained variances (X-expl) are shown on inferior part of the figure. ■, SE strain. ●, BH strain. ▲, control group.....	91
<b>Figura 17</b>	PCA plot showing the differentiation between BH and SE eggs, cercariae and miracidia of <i>S. mansoni</i> .....	92

## LISTA DE TABELAS

<b>Tabela 1</b>	Lipid chemical markers identified via MALDI-MSI and ESI-MS of <i>S. mansoni</i> adult worms (positive ion mode). Identification is based on MS/MS data, exact mass of each compound and Lipid Maps and METLIN databases.....	45
<b>Tabela 2</b>	Lipid chemical markers identified via MALDI-MSI of <i>S. mansoni</i> adult worms (positive ion mode).....	64
<b>Tabela 3</b>	Lipid chemical markers identified via HR-FTMS of <i>S. mansoni</i> eggs, miracidia and cercariae; and mice's urine infected or not by <i>S. mansoni</i> (positive ion mode). Identification is based on the comparison between the exact and theoretical masses of each compound and Lipid Maps and METLIN databases.....	93

## INTRODUÇÃO GERAL

### **Esquistossomose**

A esquistossomose, inicialmente conhecida como bilharzíase, é uma infecção intravascular causada pelo trematódeo de gênero *Schistosoma*. Cinco espécies desse gênero apresentam importância epidemiológica: *Schistosoma mansoni*, *S. japonicum*, *S. mekongi*, *S. intercalatum*, e *S. haematobium*. No entanto, somente *S. mansoni* é encontrado no Brasil (Gryseels, Polman, Clerinx, & Kestens, 2006).

A Organização de Saúde Mundial (OSM) estimou que mais de 200 milhões de pessoas na África, Ásia, América Latina e Caribe possuem esquistossomose, e que mais de 700 milhões de pessoas são expostas à infecção nesses três continentes. Entre os indivíduos infectados, no mínimo 10% apresentam a forma severa da doença, sendo que 50-60%, ou seja, mais de 100 milhões de pessoas apresentam manifestações clínicas. Tais índices fazem da esquistossomose um importante problema para a saúde pública mundial (World Health Organization, 2011). Mais especificamente no Brasil, a esquistossomose causada pelo *S. mansoni* afeta entre 2,5 e 6 milhões de pessoas e mais de 25 milhões são expostas ao risco de infecção (Ministério da Saúde Brasil, 2011).

O ciclo de vida do *S. mansoni* já é bem estabelecido. O ovo mede cerca de 150 µm e é eliminado nas fezes do homem. Quando em contato com a água, os ovos eclodem originando miracídios e parasitam o hospedeiro intermediário: um caramujo da espécie *Biomphalaria glabrata*. No caramujo, o miracídio se

desenvolve, dando origem a cercárias. Um miracídio pode dar origem a 100.000 cercárias. Na água, as cercárias penetram a pele do homem utilizando uma enzima proteolítica elastase, que é produzida em sua região frontal. Após a penetração, as cercárias perdem a cauda bifurcada e transformam-se em esquistossômulos, os quais residem por 72 h na pele antes da entrada nos vasos sanguíneos. Após passagem pelo pulmão, coração, e artérias mesentéricas, os esquistossômulos migram para o sistema porta. A maturação sexual ocorre após cerca de 30 dias da penetração, originando vermes machos e fêmeas. Os vermes adultos possuem um corpo cilíndrico de 7 a 20 mm de comprimento, com duas ventosas terminais, tegumento complexo, trato digestivo cego e órgãos reprodutores. Os vermes machos possuem uma fenda, ou canal ginecofórico, que envolve o corpo fino e longo da fêmea. A produção de ovos se inicia 4 a 6 semanas após a infecção e é contínua durante toda a vida do verme, que pode durar até 15 anos no hospedeiro definitivo. Fêmeas de *S. mansoni* produzem centenas de ovos diariamente, sendo depositados no lúmen venoso. Muitos ovos atravessam a mucosa intestinal e saem nas fezes; outros são depositados na mucosa e tecidos, como o fígado. Essa deposição ativa a resposta imune do hospedeiro e é responsável pela patologia associada à esquistossomose (Gryseels et al., 2006; Ross et al., 2002).

## **Diagnóstico da esquistossomose mansônica**

O diagnóstico de esquistossomose é dado por um conjunto de exames clínicos e laboratoriais. As ferramentas mais utilizadas para diagnóstico clínico são (i) ultrassonografia, para monitoramento dos órgãos afetados pela esquistossomose (Homeida et al., 1988); (ii) eco-doppler-cardiografia, para verificação de hipertensão portal e pulmonar (Bethlem et al., 1997) e (iii) endoscopia digestiva alta, na qual são observadas varizes gastroesofágicas (Camacho-Lobato & Borges, 1998). Para pacientes com sintomas típicos de esquistossomose e diagnóstico laboratorial negativo, a biópsia da mucosa retal também pode ser uma opção para a detecção de ovos (Gray et al., 2011).

Entre as investigações laboratoriais, a detecção e contagem de ovos nas fezes por microscopia é o exame padrão para diagnóstico de esquistossomose mansônica. Para isso, são utilizados métodos de isolamento de ovos, como Kato-Katz (Katz et al., 1972) e Lutz (Lutz, 1919). Ovos de *S. mansoni* são característicos (alongados e com espinho lateral) e de fácil visualização por microscopia. No entanto, o início da liberação de ovos pelo verme adulto demora mais de duas semanas. Além disso, essa liberação não é constante, aumentando as chances de resultados falso-negativos, principalmente nas fases iniciais da doença. Embora esse método de detecção apresente 100% de especificidade, sua sensibilidade varia de acordo com a prevalência e incidência da infecção (Gryseels et al., 2006; Ross et al., 2002).

Um método mais específico e sensível também utilizado para diagnóstico da esquistossomose é a PCR, onde o DNA do esquistossomo é amplificado a

partir das fezes e/ou soro. Embora seja capaz de diagnosticar a esquistossomose em qualquer fase da doença, é uma metodologia que exige grande preparo amostral e o rendimento inicial de DNA é extremamente baixo (Gray et al., 2011).

Métodos indiretos também podem ser utilizados para diagnóstico da esquistossomose, como detecção de antígenos do esquistossomo por anticorpos, imunofluorescência e ELISA (*Enzyme-Linked Immunosorbent Assay*). Embora técnicas indiretas sejam utilizadas em circunstâncias específicas, a aplicação é limitada. Comercialmente, kits de imunodiagnóstico disponíveis são menos sensíveis e menos específicos que os múltiplos exames fecais; além de possuir reatividade cruzada com antígenos de outros helmintos (Gray et al., 2011).

## **Tratamento da Esquistossomose**

Até o momento, Praziquantel (PZQ) é o fármaco mais utilizado para o tratamento de todas as formas de esquistossomose. Outros fármacos, como a oxamniquina e metrifonato, são eficientes somente contra uma espécie de esquistossoma e não possuem tanta disponibilidade no mercado (Cioli & Pica-Mattoccia, 2003).

A dose recomendada de PZQ é 40 a 60 mg/kg do peso corporal, sendo a menor dose geralmente utilizada em infecções por *S. mansoni*. Apesar de efetivo, PZQ apresenta, em média, 60% de cura da esquistossomose e possui baixa efetividade contra estágios imaturos do parasita (Danso-Appiah, Utzinger, Liu, & Olliaro, 2008; Gönnert & Andrews, 1977; Pica-Mattoccia & Cioli, 2004; Sabah, Fletcher, Webbe, & Doenhoff, 1986).

Embora o mecanismo de ação de PZQ seja estudado há vários anos, o conhecimento exato da ação do fármaco ainda não foi esclarecido. Em contraste, dados fisiológicos e morfológicos do verme em resposta a PZQ tem sido amplamente descritos, como a rápida captura de íons de cálcio ( $\text{Ca}^{2+}$ ), presença de vacúolos e formação de bolhas na superfície do verme (Doenhoff, Cioli, & Utzinger, 2008).

## **Biomarcadores**

Os biomarcadores possuem aplicação clínica com objetivos que variam entre a compreensão de mecanismos moleculares, diagnóstico, monitoramento da evolução de uma doença e até da resposta terapêutica e/ou toxicológica. Podem se apresentar em diferentes formas e, portanto, diferentes estratégias podem ser adotadas para suas descobertas (Rifai et al., 2006).

Apesar do grande interesse industrial, acadêmico e clínico, e do amplo investimento na área, a velocidade de criação de diagnósticos envolvendo biomarcadores ainda é lenta. As razões deste fenômeno são o longo e difícil caminho a partir da descoberta ao teste clínico. Etapas como descoberta, qualificação, verificação, otimização, validação clínica e comercialização estão entre os processos essenciais para a obtenção de um novo biomarcador. Entretanto, a presença de dificuldades relacionadas ao tipo de amostra é comum durante essa busca. Por exemplo, i) a complexidade dos biofluidos; ii) a baixa abundância relativa de muitos marcadores específicos de doenças; e iii) a variabilidade das manifestações das doenças nos seres humanos.

No Brasil, ainda é escasso o emprego de estratégias metabolômicas como ferramenta para a pesquisa de biomarcadores, principalmente em metabólitos celulares de baixo peso molecular. Portanto, o uso da metabolômica para a identificação de biomarcadores clínicos torna-se indispensável. Assim, aliar a metabolômica com a descoberta, qualificação, verificação, e validação de biomarcadores torna-se uma tarefa de suma importância científica e tecnológica. Além disso, moléculas como lipídeos, esfingolipídios e ceramidas podem ser bons biomarcadores, tanto para o entendimento de mecanismos moleculares, como potencial foco terapêutico em fisiopatologias (Kaddurah et al., 2008).

## **Metabolômica**

A metabolômica é uma importante plataforma bioquímica para o estudo de mecanismos e identificação de biocomponentes existentes nos organismos em diferentes condições fisiopatológicas, revelando potenciais biomarcadores e ampliando a compreensão da etiopatogenia de doenças (Kaddurah et al., 2008). Seu conceito básico é definido como análise das moléculas do metaboloma, que é o conjunto dos produtos finais resultante das atividades enzimáticas. Em outras palavras, é o conjunto das moléculas de baixo peso molecular geradas pelo metabolismo primário e intermediário (Kaddurah et al., 2008).

Uma vez conhecida a composição dos metabólitos, é possível prever, por exemplo, a ativação de determinados genes (nos casos de regulação conhecida), entender os mecanismos moleculares, avaliar o risco imediato para determinadas doenças de forma a poder intervir quando ainda em estágio subclínico, ou

identificar novos biomarcadores de doenças e assim obter um diagnóstico (Sabatine et al., 2005).

As estratégias metabolômicas para identificação de biomarcadores podem ser subdivididas em i) *Metabolic profiling*: Identificação e quantificação de um número pré-definido de metabólitos, que geralmente é relacionado a uma via metabólica específica; ii) *Metabolic fingerprint*: análises rápidas cuja função é fornecer a classificação da amostra. Também utilizada como importante ferramenta de *screening* para diferenciar estados biológicos (caso/ controle, doença/saúde); iii) *Metabolic footprint*: análise dos metabólitos secretados/excretados por um organismo; iv) *Metabolite target analysis*: análise quantitativa e/ou qualitativa de um ou de vários metabólitos relacionados a uma reação metabólica específica; v) *Metabonomics*: análise quantitativa de metabólitos em resposta a uma lesão/perturbação (doença ou tratamento terapêutico) ou a modificação genética. Devido às várias estratégias dispostas em análise metabolômica é possível acessar um número enorme de estados fisiopatológicos e as vias bioquímicas para melhor entendê-los, além de auxiliar novas descobertas na área de medicina translacional (Kaddurah et al., 2008).

## **Técnicas utilizadas em metabolômica**

Análises metabolômicas podem ser realizadas utilizando-se ferramentas como a cromatografia com alto poder de separação e/ou ressonância magnética nuclear e espectrometria de massas (MS), seguida de tratamento de dados com programas quimiométricos (Kaddurah et al., 2008). Tais técnicas aplicadas ao

metaboloma poderão futuramente auxiliar no diagnóstico clínico no contexto mundial. A cromatografia é um método que, embora seja difícil de identificar os componentes separados, auxilia na eliminação de interferentes e conserva a estrutura de cada composto isolado (Kaddurah et al., 2008). Por outro lado, exige tempo de preparação de amostra e análise. Quando acoplada a técnicas analíticas, como MS, é capaz de separar diferentes classes de lipídeos, sem problemas de supressão de íons, e permite a resolução de espécies moleculares isobáricas, com massas moleculares idênticas e estruturas moleculares diferentes. Ainda, é possível quantificar com múltiplos padrões internos e externos (Postle, 2012; Davis et al., 2008).

Já a espectrometria de massas gradativamente minimiza os desafios da detecção e quantificação de substâncias em matrizes complexas (como os fluidos biológicos). Tal ferramenta é capaz de analisar simultaneamente grupos de analitos em volumes pequenos de amostra e em poucos minutos. Diversas técnicas têm sido desenvolvidas para melhorar a precisão, resolução e mobilidade dos íons no espectrômetro de massas, tais como o Thermo LTQ-Orbitrap, FT-ICR (*Fourier Transformed Ion Cyclotron Resonance*) e Waters Synapt G2 (Postle 2012; Davis et al 2008). No entanto, exigem etapas de extração e purificação, levando a perda da distribuição de lipídeos na amostra analisada (Van Goor et al 1986). Por outro lado, técnicas de imageamento químico por espectrometria de massas (MSI) são capazes de detectar e localizar lipídeos de forma eficaz, como SIMS (*Secondary Ion Mass Spectrometry*), DESI (*Desorption Electrospray Ionization*), LAESI (*Laser Ablation Electrospray Ionization*), e MALDI (*Matrix-Assisted Laser Desorption/Ionization*). De todas essas abordagens, MALDI-MSI é a mais comum

para imageamento de lipídeos (Goto-Inoue et al., 2011). Todo esse aprimoramento possibilita a aplicação da espectrometria de massas, com grande confiabilidade e sensibilidade, em diversos campos científicos e tecnológicos da atualidade, como estudos de compostos nas áreas da química analítica e ambiental, da bioquímica, da biologia e da medicina (Kaddurah et al., 2008).

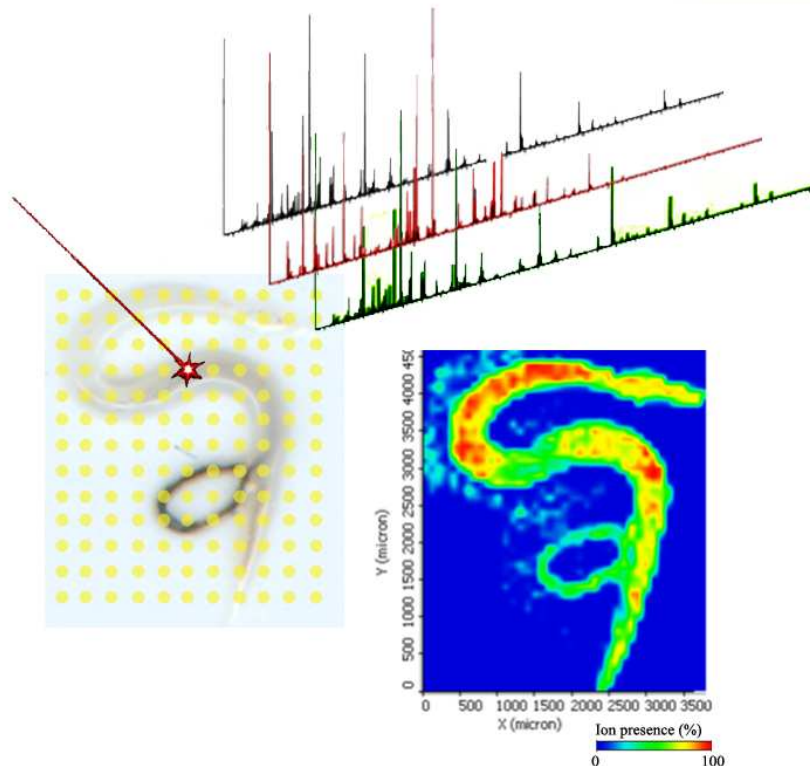
### **MALDI-MSI (*Mass Spectrometry Imaging*)**

Ao longo da última década, a metabolômica tornou-se um complemento indispensável às análises de quase todos os aspectos das ciências da vida. Estes incluem a elucidação de processos celulares e a descoberta e avaliação de compostos farmacêuticos. Como ferramenta analítica, a espectrometria de massas tornou-se essencial para a investigação destes processos moleculares. Novos avanços em MS oferecem agora a oportunidade para estudos na investigação de interações moleculares no tecido intacto. Ao contrário dos estudos realizados por décadas, hoje é possível aproveitar a especificidade molecular oferecida pela MS. Em particular, MALDI-MSI permite a análise espacial da distribuição de metabólitos diretamente em amostras biológicas, sem qualquer conhecimento prévio ou a necessidade de reagentes específicos (Goto-Inoue et al., 2011).

MALDI-MSI é um método de ionização capaz de ionizar analitos na superfície através de pulsos de laser. A amostra é misturada a uma matriz ou nanopartícula, que absorve a luz no comprimento de onda do laser (Figura 1), sendo capaz de ionizar biomoléculas com razão massa/carga ( $m/z$ ) menores que

1000 Da a maiores que 100 kDa (Svatos, 2010; Yates, 1998). Embora possua algumas desvantagens em termos de resolução espacial, MALDI é considerada a melhor técnica atualmente disponível para imageamento de lipídeos. É uma técnica rápida, onde um dos fatores mais relevantes é a frequência do laser. A maioria dos instrumentos de MALDI é equipada com lasers de 1000 Hz (Goto-Inoue et al., 2011).

*Figura 1. Incidência de laser sobre amostra recoberta com matriz. Varredura da amostra pelo laser gera espectros em tempo real e imagem química.*



Dois outros fatores são de extrema importância para a análise de imageamento: (i) a preparação da amostra e (ii) a escolha da matriz apropriada. É necessário otimizar o procedimento de preparação de acordo com as

características químicas e físicas de cada analito. Etapas como fixação do material, tipo de secção e estocagem possuem grande influência na obtenção de sinais de biomoléculas durante o imageamento. Além disso, a eficiência da ionização também depende parcialmente da espessura da secção do tecido (Sugiura et al., 2006). Em geral, secções de 5 a 20 µm são preparadas para análises de moléculas de baixo peso molecular. Enquanto secções de 2 a 5 µm são recomendadas para análises de moléculas de alto peso molecular (3-21 kDa) (Goodwin et al., 2008).

Para lipídeos e pequenos metabólitos, geralmente são utilizadas matrizes como 2,5-diidroxibenzóico (DHB) e 9-aminoacridina (9-AA) (McDonnell & Heeren, 2007). Em MALDI-MSI, analitos devem ser co-cristalizados com matrizes para serem ionizados. O método de aplicação da matriz também influencia a eficiência de extração do analito. Há várias maneiras de aplicação da matriz em uma secção, tais como deposição, spray e sublimação. Comparado com outros métodos, a deposição da solução de matriz aumenta a sensibilidade do sinal, mas diminui a resolução espacial (Aerni et al 2006). Já a aplicação por spray permite que a amostra seja revestida com cristais relativamente pequenos de forma homogênea. Entretanto, tal metodologia exige certos cuidados. Segundo Agar e colaboradores (2007), se há um excesso de matriz borrifada na amostra a ser analisada, cristais não homogêneos podem ser formados com analitos que migraram de sua localização inicial. Por outro lado, se há pouca solução de matriz na amostra, analitos podem não ser adequadamente extraídos da secção.

Para reduzir a limitação causada pelo tamanho dos cristais, foi criado um

método de aplicação de matriz por sublimação (Hankin et al 2007), onde é possível revestir a amostra uniformemente em poucos minutos e sem utilização de solventes. Essa metodologia aumenta o sinal do analito pela formação de finos microcristais de vapores condensados, mas requer uma instrumentação especial (Vrkoslav et al 2010).

A técnica de MALDI-MSI permite, ainda, diferenciar moléculas de mesma  $m/z$ , através do imageamento MS/MS. Assim, é possível separar cada íon derivado do seu fragmento específico (Sugiura & Setou, 2010). Além disso, a combinação da separação por mobilidade de íons com MALDI-MSI fornece uma única dimensão de separação, produzindo imagens sem interferência de gradiente de íons com massas similares, removendo a ambiguidade de experimentos de imageamento e levando a uma localização mais precisa dos compostos de interesse (Stauber et al, 2010, Jackson et al, 2007, McLean et al, 2007).

### **ESI-MS de alta resolução (HR-FTMS-Orbitrap)**

Na ionização por *electrospray* (ESI), as substâncias da solução analítica são protonadas ou desprotonadas, formando cátions ou ânions. Esta solução é então nebulizada através de um tubo capilar onde se aplica uma alta voltagem. Devido à ação deste potencial aplicado no capilar e dos gases de dessolvatação e nebulização, o solvente presente nas gotículas é evaporado restando assim a molécula protonada ou desprotonada na fase gasosa. Entre as características da

ionização por *electrospray*, pode-se citar a baixa energia dos íons formados e a possibilidade da formação de íons multicarregados (Hardman & Makarov, 2003).

Acoplados à ferramenta ESI, podem ser utilizados diferentes tipos de analisadores. Para análise de amostras complexas por MS, a espectrometria de massas em tandem ( $MS^n$ ), bem como equipamentos de alta resolução e alta acurácia, podem facilitar a detecção de um ou mais analitos particulares. Por exemplo, o Orbitrap se destaca pela alta resolução (acima de 150 000), grande capacidade de carga espacial, alta acurácia de massa (na faixa de partes por milhão - ppm) e uma gama de massa/carga ( $m/z$ ) de no mínimo 6000. Nesse tipo de equipamento, os íons são transferidos da fonte de ESI para três quadrupolos. O terceiro, pressurizado a menos de  $10^{-3}$  Torr com colisão de gás, age como um acumulador de íons. A colisão de íons desacelera-os, fazendo com que se aglomerem no final do quadrupolo. Esse grupo de íons entra no analisador Orbitrap, onde se movem em volta de um eletrodo central para análise das massas (Hu et al., 2005).

Todas estas características fazem com que a tecnologia de espectrometria de massas de alta resolução, em especial do Orbitrap, seja uma importante ferramenta para as estratégias metabolômicas na busca de biomarcadores. Por permitir a clara visualização no espectro de compostos com razão  $m/z$  próximas, a alta resolução facilita a identificação de biomoléculas com grande confiabilidade.

## REFERÊNCIAS BIBLIOGRÁFICAS

- Aerni, H.R., Cornett, D.S., Caprioli, R.M. 2006. Automated acoustic matrix deposition for MALDI sample preparation. *Anal. Chem.* 78: 827-834.
- Agar, N.Y., Yang, H.W., Carroll, R.S., Black, P.M., Agar, J.N. 2007. Matrix solution fixation: histology-compatible tissue preparation for MALDI mass spectrometry imaging. *Anal. Chem.* 79: 7416-7423.
- Bethlem, E. P., Schettino, G. D. P. P., & Carvalho, C. R. R. 1997. Pulmonary schistosomiasis. *Current opinion in pulmonary medicine*, 3(5): 361-365.
- Camacho-Lobato, L., & Borges, D. R. 1998. Early liver dysfunction in schistosomiasis. *Journal of hepatology*, 29(2): 233-240.
- Cioli, D., & Pica-Mattoccia, L. 2003. Praziquantel. *Parasitology Research*, 90(1): S3-S9.
- Danso-Appiah, A., Utzinger, J., Liu, J., & Olliaro, P. 2008. Drugs for treating urinary schistosomiasis. *Cochrane Database Syst Rev*, 3.
- Davis, B., Koster, G., Douet, L.J. et al. 2008. Electrospray ionization mass spectrometry identifies substrates and products of lipoprotein-associated phospholipase A2 in oxidized human low density lipoprotein. *J Biol Chem.* 283: 6428-6437.
- Doenhoff, M. J., Cioli, D., & Utzinger, J. 2008. Praziquantel: mechanisms of action, resistance and new derivatives for schistosomiasis. *Current opinion in infectious diseases*, 21(6): 659-667.
- Gönnert, R., & Andrews, P. 1977. Praziquantel, a new broad-spectrum antischistosomal agent. *Zeitschrift für Parasitenkunde*, 52(2): 129-150.
- Goodwin, R.J., Pennington, S.R., Pitt, A.R. 2008. Protein and peptides in pictures: imaging with MALDI mass spectrometry. *Proteomics*. 8: 3785-3800.
- Goto-Inoue, N., Hayasaka, T., Zaima, N., Setou, M. 2011. Imaging mass spectrometry for lipidomics. *Biochimica et Biophysica Acta*. 1811: 961-969.
- Gray, D. J., Ross, A. G., Li, Y.-S., & McManus, D. P. 2011. Diagnosis and management of schistosomiasis. *BMJ: British Medical Journal*, 342.
- Gryseels, B., Polman, K., Clerinx, J., & Kestens, L. 2006. Human schistosomiasis. *Lancet*, 368(9541): 1106-1118.
- Gryseels, B., Polman, K., Clerinx, J., & Kestens, L. 2006. Human schistosomiasis. *Lancet*, 368(9541): 1106-1118.
- Hankin, J.A., Barkley, R.M., Murphy, R.C. 2007. Sublimation as a method of matrix application for mass spectrometric imaging. *J. Am. Soc. Mass Spectrom.* 18: 1646-1652.
- Hardman, M., & Makarov, A. A. 2003. Interfacing the orbitrap mass analyzer to an electrospray ion source. *Analytical chemistry*, 75(7): 1699-1705.

- Homeida, M., Abdel-Gadir, A. F., Cheever, A. W., Bennett, J. L., Arbab, B., Ibrahium, S. Z., Abdel-Salam, I. M., Dafalla, A. A., & Nash, T. E. 1988. Diagnosis of pathologically confirmed Symmers' periportal fibrosis by ultrasonography: a prospective blinded study. *The American journal of tropical medicine and hygiene*, 38(1): 86-91.
- Hu, Q., Noll, R. J., Li, H., Makarov, A., Hardman, M., & Graham Cooks, R. 2005. The Orbitrap: a new mass spectrometer. *Journal of mass spectrometry*, 40(4): 430-443.
- Jackson, S.N., Ugarov, M., Egan, T., Post, J.D., Langlais, D., Schultz, J.A., Woods, A.S. 2007. MALDI-ion mobility-TOFMS imaging of lipids in rat brain tissue. *J. Mass Spectrom.* 42: 1093-1098.
- Kaddurah-Daouk, R., Kristal, B.S., Weinshilboum, R.M. 2008. Metabolomics: a global biochemical approach to drug response and disease. *Annu. Rev. Pharmacol. Toxicol.*, 48: 653-683.
- Katz, N., Chaves, A., & Pellegrino, J. 1972. A simple device for quantitative stool thick-smear technique in Schistosomiasis mansoni. *Revista do Instituto de Medicina Tropical de São Paulo*, 14(6): 397.
- Lutz, A. 1919. Schistosum mansoni and schistosomatosis observed in Brazil. *Memórias do Instituto Oswaldo Cruz*, 11(1): 121-155.
- McDonnell, L.A., Heeren, R.M. 2007. Imaging mass spectrometry. *Mass Spectrom. Rev.* 26: 606-643.
- McLean, J.A., Ridenour, W.B., Caprioli, R.M. 2007. Profiling and imaging of tissues by imaging ion mobility-mass spectrometry. *J. Mass Spectrom.* 42: 1099-1105.
- Ministério da Saúde Brasil, 2011. Esquistossomose. Site: <http://bvsms.saude.gov.br/>. Acessado em setembro de 2014.
- Pica-Mattoccia, L., & Cioli, D. 2004. Sex-and stage-related sensitivity of *Schistosoma mansoni* to in vivo and in vitro praziquantel treatment. *International journal for parasitology*, 34(4): 527-533.
- Postle, A.D. 2012. Lipidomics. *Curr Opin Clin Nutr Metab Care*, 15: 127-133.
- Rifai, N., Gillette, M.A., Carr, S.A. 2006. Protein biomarker discovery and validation: the long and uncertain path to clinical utility. *Nature Biotechnology*, 24: 971-983.
- Ross, A. G., Bartley, P. B., Sleigh, A. C., Olds, G. R., Li, Y., Williams, G. M., & McManus, D. P. 2002. Schistosomiasis. *N Engl J Med*, 346(16): 1212-1220.
- Sabah, A., Fletcher, C., Webbe, G., & Doenhoff, M. 1986. *Schistosoma mansoni*: Chemotherapy of infections of different ages. *Experimental parasitology*, 61(3): 294-303.
- Sabatine, M.S., Liu, E., Morrow,D.A., Heller, E., McCarroll, R., Wiegand, R., Berriz, G.F., Roth, F.P., Gerszten, R.E. 2005. Metabolomic identification of novel biomarkers of myocardial ischemia. *Circulation*, 112: 3868-3875.

- Stauber, J., MacAleese, L., Franck, J., Claude, E., Snel, M., Kaletas, B.K., Wiel, I.M., Wisztorski, M., Fournier, I., Heeren, R.M. 2010. On-tissue protein identification and imaging by MALDI-ion mobility mass spectrometry. *J.Am. Soc.Mass Spectrom.* 21: 338-347.
- Sugiura, Y., Shimma, S., Setou, M. 2006. Thin sectioning improves the peak intensity and signal-to-noise ratio in direct tissue mass spectrometry. *J. Mass Spectrom. Soc. Jpn.* 54: 1-4.
- Sugiura, Y., Shimma, S., Setou, M. 2006. Thin sectioning improves the peak intensity and signal-to-noise ratio in direct tissue mass spectrometry. *J. Mass Spectrom. Soc. Jpn.* 54: 1-4.
- Svatos, A. 2010. Mass spectrometric imaging of small molecules. *Trends Biotechnol.* 28: 425-434.
- Van Goor, H., Gerrits, P., & Grond, J. 1986. The application of lipid-soluble stains in plastic-embedded sections. *Histochemistry*, 85(3): 251-253.
- Vrkoslav, V., Muck, A., Cvacka, J., Svatos, A. 2010. MALDI imaging of neutral cuticular lipids in insects and plants. *J. Am. Soc. Mass Spectrom.* 21: 220-231.
- World Health Organization. Helminth control in school-age children: a guide for managers of control programmes. 2th ed. Geneva, 2011.
- Yates, J.R. 1998. Mass spectrometry and the age of the proteome. *J. Mass Spectrom.* 33: 1-19.

## **OBJETIVOS**

### **Objetivo Geral**

Implementação de estratégias e plataformas analíticas, utilizando como ferramenta analítica a Espectrometria de Massas por Imagem e de Alta Resolução, na caracterização química de *S. mansoni*. Tais dados poderão futuramente ser utilizados como alvos terapêuticos para desenvolvimento de novos fármacos e auxiliar na compreensão de potenciais vias metabólicas envolvidas.

### **Objetivos Específicos**

- Caracterizar separadamente ambos os sexos de vermes adultos de *S. mansoni* *in vitro*, comparando duas cepas brasileiras de diferentes regiões, SE e BH.
- Caracterizar separadamente ambos os sexos de vermes adultos de *S. mansoni* *in vivo*, tratados ou não com PZQ.
- Localizar os marcadores químicos no corpo dos vermes adultos por imageamento utilizando MALDI-MSI.
- Caracterizar separadamente diferentes estágios do ciclo de vida de *S. mansoni*, como ovos, miracídio e cercária, comparando as cepas SE e BH.
- Caracterizar e diferenciar urina de camundongos infectados ou não com as cepas de esquistossomose SE e BH, separadamente, possibilitando futuro rápido diagnóstico alternativo de *S. mansoni*.

## **CAPÍTULO I**

**Espectrometria de Massas por Imagem: uma  
nova visão na diferenciação de cepas de  
*Schistosoma mansoni.***

# **Mass Spectrometry Imaging: a new vision in differentiating *Schistosoma mansoni* strains.**

**Mônica Siqueira Ferreira<sup>1</sup>, Diogo Noin de Oliveira<sup>1</sup>, Rosimeire Nunes de Oliveira<sup>2</sup>, Silmara Marques Allegretti<sup>2</sup>, Aníbal Eugênio Vercesi<sup>3</sup>, Rodrigo Ramos Catharino<sup>1\*</sup>**

**1** Innovare Biomarkers Laboratory, Medicine and Experimental Surgery Nucleus, University of Campinas, Campinas, São Paulo, Brazil. **2** Biology Institute, Animal Biology Department, University of Campinas, Campinas, São Paulo, Brazil. **3** Bioenergetics Laboratory, Medicine and Experimental Surgery Nucleus, University of Campinas, Campinas, São Paulo, Brazil.

\*Corresponding author. Tel.: +55 19 3521 9138.  
E-mail address: rrc@fcm.unicamp.br (R.R. Catharino).

## **ABSTRACT**

Schistosomiasis is a neglected disease with large geographic distribution worldwide. Among the several different species of this parasite, *S. mansoni* is the most common and relevant one; its pathogenesis is also known to vary according to the worms' strain. High parasitical virulence is directly related to granulomatous reactions in the host's liver, and might be influenced by one or more molecules involved in a specific metabolic pathway. Therefore, better understanding the metabolic profile of these organisms is necessary, especially for an increased potential of unraveling strain virulence mechanisms and resistance to existing treatments. In this report, MALDI-MSI and the metabolomic platform were employed to characterize and differentiate two Brazilian *S. mansoni* strains: males and females from Belo Horizonte (BH) and from Sergipe (SE). By performing direct analysis, it is possible to distinguish the sex of adult worms, as well as identify the spatial distribution of chemical markers. Phospholipids, diacylglycerols and triacylglycerols were located in specific structures of the worms' bodies, such as tegument, suckers, reproductive and digestive systems. Lipid profiles were found to be different both between strains and males or females, giving specific metabolic fingerprints for each group. This indicates that biochemical characterization of adult *S. mansoni* may help narrowing-down the investigation of new therapeutic targets according to worm composition, molecule distribution and, therefore, aggressiveness of disease.

**Keywords:** *Schistosoma mansoni*; sex differentiation; strains; MSI; parasitomics.

## INTRODUCTION

Schistosomiasis is an intravascular infection caused by a trematode of the genus *Schistosoma* [1]. There are five *Schistosoma* species that infect humans: *S. mansoni*, *S. japonicum*, *S. mekongi*, *S. intercalatum*, and *S. haematobium*. Among these, only *S. mansoni* is found in Brazil. This species is the major causative agent of human schistosomiasis, and has the largest geographic distribution, affecting thousands of people in Africa, Middle East, South America, and the Caribbean [1]. This is the main reason why there has been an increasing interest and extensive studies concerning this matter in recent years [2, 3].

The regular cycle of schistosomiasis transmission happens when human skin is exposed to fresh water infested with *Biomphalaria* sp. snails – intermediate host – infected with cercariae. After penetration of cercariae through the skin, they lose their tails and transform into the schistosomula which reside in the skin for up to 72 hours before entering a blood vessel. After a lung passage, the parasites migrate to the portal venous system, where they mature into male and female worms and deposit hundreds of eggs daily [1, 3]. The adult worms have a cylindrical body of 7 to 20 mm in length, with complex tegument and separated sexes [4]. The male's body forms a groove, also called gynaecophoric channel, in which it holds the longer and thinner female [5].

Previous studies suggest that different strains present distinct characteristics in pre-patent period, infectivity, pathogenicity, eggs' kinetics in the feces, liver and the intestinal wall, morphological differences between the adult worms, as well as

differences in susceptibility to treatment [6]. Yoshioka, *et al.* [7] conducted a comparative study of the pathogenesis of three strains of *Schistosoma* from different Brazilian geographical regions: SR (Santa Rosa, Campinas, SP), BH (Belo Horizonte, MG) and SJ (São José dos Campos, SP). The obtained data revealed that the SR strain is less pathogenic than the other two, since it yielded fewer worms and shed eggs and had a lower number and of granulomas and smaller granuloma size in the liver and intestine.

Considering the high prevalence and incidence of schistosomiasis, the fact that treatment is based only on a single drug and factors regarding tolerance and resistance, there is an urge for better understanding the bidirectional host-parasite relationship in order to identify potential new drug targets and new forms of control.

Some studies have recently employed modern analytical approaches for chemical characterizations of adult schistosomes using a whole worm extract along with chromatographic techniques, such as thin-layer chromatography (TLC), gas chromatography coupled with mass spectrometry (GC-MS) and high performance liquid chromatography (HPLC) [8, 9]. Others have employed matrix-assisted laser desorption/ionization mass spectrometry (MALDI-MS) as the main analytical tool [10], but its variation, mass spectrometry imaging (MSI) [11] has never been performed. MSI was developed to identify the spatial distribution of compounds in any physical sample, such as tissue sections [12], drug tablets [13], cosmetic products [14] and now whole intact parasites. Furthermore, other ionization methods also allow to visualize the spatial distribution of molecules, namely Secondary Ionization Mass Spectrometry (SIMS) [15], Desorption Electrospray Ionization (DESI) [16] and Laser Ablation Electrospray Ionization (LAESI) [17].

Despite these previous studies in *S. mansoni* composition and characterization [9, 10], compound distribution was still unknown. For that reason, the present work uses a combination of MSI and multivariate data analysis to characterize and differentiate two *S. mansoni* strains – BH and SE – and is also the first paper to discuss any biochemical aspect on the SE strain of this parasite. This report demonstrates that it is possible to determine the sex of adult worms and identify the spatial distribution of chemical markers using MALDI-MSI technology, potentially helping in the search for new therapeutic targets in the development of antischistosomal drugs.

## MATERIAL AND METHODS

**Ethics statement.** This study was carried out in strict accordance with the recommendations in the Guide for the Care and Use of Laboratory Animals. The protocol was approved by the International Ethics Commission for the Use of Animals (CEUA/ICCLAs, protocol nº 2170-1).

**Animals and parasite maintenance.** *Schistosoma mansoni* (BH) strain - from Belo Horizonte, MG, Brazil - and (SE) strain - from Ilha das Flores, SE, Brazil were used throughout this study. The strains were hosted in *Biomphalaria glabrata* freshwater snails as intermediates for the parasite early life cycle at the Department of Animal Biology, Biology Institute, University of Campinas (UNICAMP). Swiss/SPF female mice, weighing  $20\pm5$  g and 4 weeks of age were used as the definitive hosts. Two groups ( $n=5$ ) were briefly exposed to an aqueous suspension containing 70 cercariae of *S. mansoni* (BH and SE). Invasion was

allowed to proceed by the tail immersion technique [18]. After infection, the mice were maintained under controlled environment (temperature between 20°C and 22°C) with daylight cycle for 60 days.

**Recovery and culture of *S. mansoni*.** After 60 days of infection, adult *S. mansoni* worms (male and female) were retrieved through perfusion of the hepatic portal system and mesenteric veins of sacrificed mice, as described by Smithers and Terry (1965) [19]. These were washed in RPMI-1640 (Nutricell®) medium supplemented with 0,05 g/L of streptomycin, 10.000 UI/mL of penicillin, 0,3 g/L of L-Glutamine, 2,0 g/L of D-Glucose, 2,0 g/L of NaHCO<sub>3</sub> and 5,958 g/L of Hepes. For preparations, an *in vitro* culture with each strain of *S. mansoni* worm couples was transferred to different wells of a culture plate containing 2 mL of the same medium. Sequentially, the plates were incubated at 37° C in a greenhouse containing 5% CO<sub>2</sub> [20]. The cultures were observed through an inverted optical microscope DM-500 (Leica®) for 72 hours prior to use.

**MALDI-MSI analysis.** All adult worms of *S. mansoni* were washed with H<sub>2</sub>O milliQ and deposited in a thin-layer chromatography (TLC) plate (Merck, Darmstadt, Germany). Matrix coating was performed using a commercial airbrush, spraying α-cyano-4-hydroxycinnamic acid (Sigma-Aldrich, Pennsylvania, USA) (10 mg/mL in 1:1 Acetonitrile/Methanol solution). Images and mass spectra were acquired in a MALDI-LTQ-XL instrument equipped with imaging feature (Thermo Scientific, California, USA). The instrument has an ultraviolet laser as ionization source and a quadrupole-ion-trap analyzing system. All data were acquired in the positive ion

mode. For image acquisition, a 50 µm raster width was selected. Fragmentation data (MS/MS) were acquired by setting the collision-induced energy (CID) to 40 eV. Helium was used as the collision gas. Each ion was fragmented in triplicates. All imaging data were then processed using ImageQuest software v.1.0.1 (Thermo Scientific, California, USA).

**Statistical analysis and chemical marker identification.** Principal Component Analysis (PCA) was performed using Unscrambler v.9.7 (CAMO Software, Trondheim, Norway). The software has clustered samples according to the relationship between *m/z* and intensity, with the results expressed as groups of samples with the same characteristics when considered these parameters. MS/MS reactions were performed with each potential chemical marker identified by PCA. Lipid MAPS online database (University of California, San Diego, CA – [www.lipidmaps.org](http://www.lipidmaps.org)) and METLIN (Scripps Center for Metabolomics, La Jolla, CA) were consulted to help guiding the choice for potential lipid markers. Their structures were later inputted in Mass Frontier software v.6.0 (Thermo Scientific, California, USA), where a number of fragments and mechanisms were modeled. Mass Frontier uses literature data and mathematical calculations to propose fragmentation mechanisms and products [21]. Structures were assigned to molecules that presented the highest number of matches between MS/MS experimental data and Mass Frontier fragments.

**High resolution ESI-MS analysis.** To confirm the chemical markers identifications, males and females of both strains were submitted to a Bligh-Dyer

extraction [22]. Lipid extracts were resuspended in 50 µL of H<sub>2</sub>O milliQ and 10 µL of the latter was diluted in 990 µL of methanol and 0,1% formic acid. Data acquisition was performed in a LTQ-XL Orbitrap Discovery instrument (Thermo Scientific, Bremen, Germany) in the positive ion mode and at the *m/z* range of 600-2000 for complex lipid identification. Structural propositions were performed using high resolution as the main parameter. Mass accuracy was calculated and expressed in terms of ppm shifts.

## RESULTS

### Metabolic fingerprint of adult worms

Male and female adult worms of two different strains- BH and SE were subjected to MALDI-MSI analysis, as described in methods. All of them presented clear differences in their spectra when compared to each other (Figure 2). Additionally, images generated by metabolic fingerprinting, i.e. total ion current, were representatively illustrated beside each spectrum (Figure 2), demonstrating the specificity in worm detection.

Furthermore, coupled *S. mansoni* worms of the SE strain also were analyzed. It was possible to detect both worms' bodies: male (clear); and female (dark) into the gynaecophoric channel (Figure 3A and 3B). Spectra of the pair were compared with single worms (SE strain). As shown in Figure 3C, most of the ions refer to male's body. However, the signal at *m/z* 825 is the only one that belongs to the female's body.

*Figure 2. Representative fingerprinting images and spectra of *Schistosoma mansoni* adult worms. The imaging represents a sum of all ions within mass range m/z 600–2000. (A) Male BH strain (MBH); (B) male SE strain (MSE); (C) female BH strain (FBH) and (D) female SE strain (FSE). Positive ion mode.*

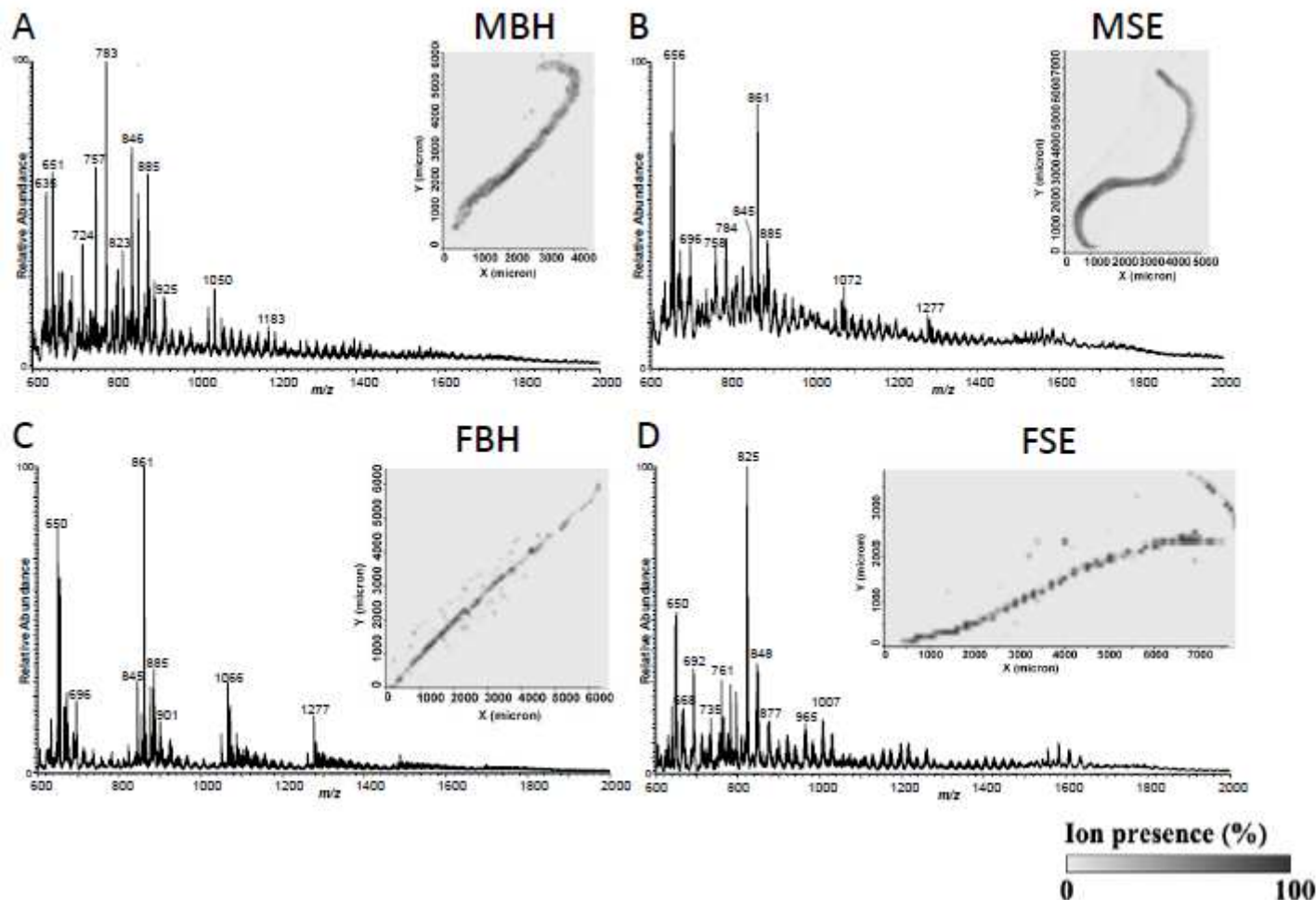
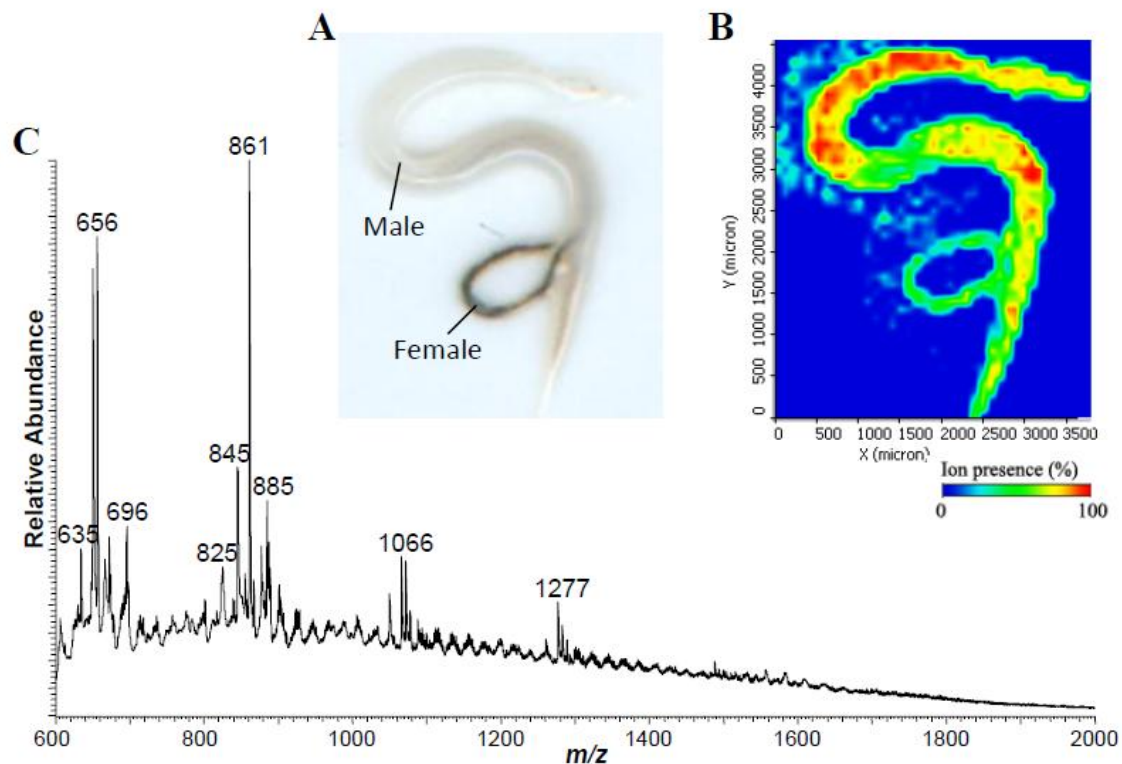


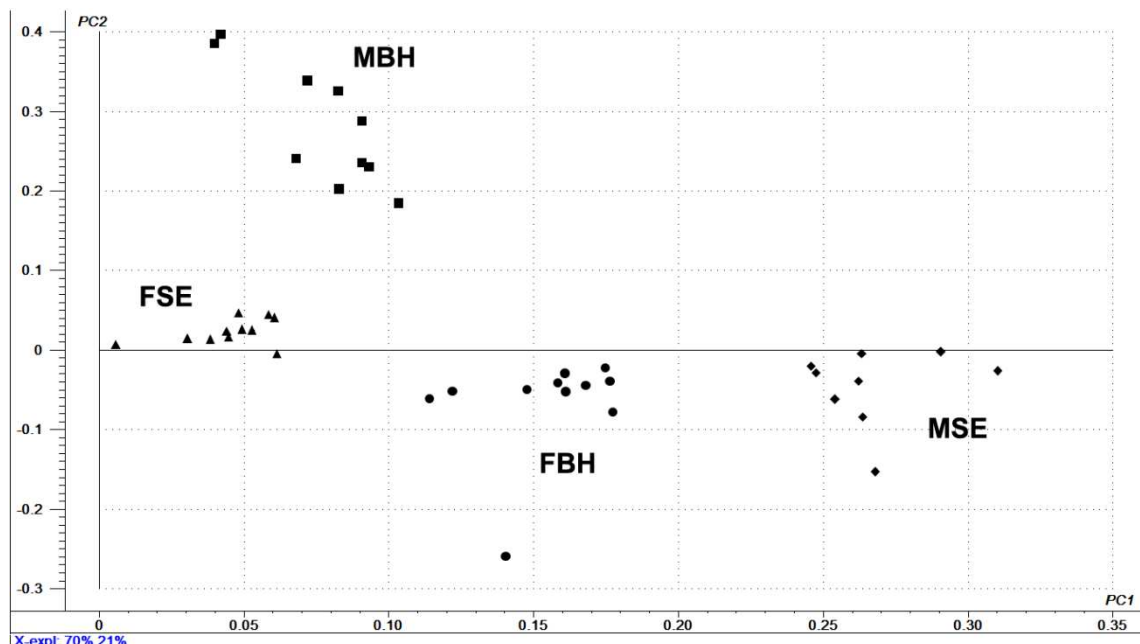
*Figure 3. Representative fingerprinting of Schistosoma mansoni adult couple worms. The imaging represents a sum of all ions within mass range m/z 600–2000. (A) Picture of worms analyzed. Gynaecophoric channel in male's body (clear) holding female's body (dark). (B) Worms image generated by MALDI-MSI instrument. Illustrative picture of fingerprinting analysis. (C) Representative fingerprinting (total ion current)spectra. Positive ion mode.*



### Statistical analysis and chemical markers identification

Statistical analysis was performed by the comparison between male and female of SE and BH strains. As shown in Figure 4, all groups were clearly separated with an accuracy of 91%. The identified ions compose the final model of optimized PCA.

*Figure 4. Principal component analysis of Schistosoma mansoni adult worms. Ion chemical markers of each group separated by principal component analysis ( $n = 10/\text{group}$ ). The explained variances ( $X\text{-expl}$ ) are shown on inferior part of the figure. ■, male BH strain (MBH); ●, female BH strain (FBH); ♦, male SE strain (MSE) and ▲, female SE strain (FSE).*



For chemical marker identification, ion fragmentation reactions (MS/MS) were performed and then compared to characteristic fragmenting patterns predicted by software, as described in the “Materials and Methods” section. High-resolution Fourier transform mass spectrometry (HR-FTMS) was also utilized at this stage, with experimental masses compared to theoretical found at METLIN database. Table 1 presents chemical markers identified in each adult worm, as well as the precursor ion fragmentation and the mass errors for each signal observed in HR-FTMS, measured in ppm (with all results presenting a deviation of less than 2 ppm).

*Table 1. Lipid chemical markers identified via MALDI-MSI and ESI-MS of *S. mansoni* adult worms (positive ion mode). Identification is based on MS/MS data, exact mass of each compound and Lipid Maps and METLIN databases.*

TAG, Triacylglycerol. PC, Phosphatidylcholine. DAG, Diacylglycerol. PA, Phosphatidic Acid. PE, Phosphoethanolamine. PI, Phosphoinositol.

Adult worm strain	m/z	MS/MS	Molecule	LM ID*	Theoretical Mass	Experimental Mass	Mass Error (ppm)	MID**
MSE	786	740, 742, 597, 768, 641, 623	[TAG(13:0/17:2/17:2) + H] <sup>+</sup>	LMGL03012730	785.66537	785.66610	0.9291488	98589
	825	781, 636, 765, 548, 592, 504, 680	[PC(17:0/22:4) + H] <sup>+</sup>	LMGP01011520	824.61638	824.61761	1.4916027	75800
	850	806, 726, 705, 661, 832, 791	[TAG(17:0/17:0/17:0) + H] <sup>+</sup>	LMGL03010031	849.79057	849.79152	1.1179225	4730
FSE	606	417, 461, 562, 435, 488, 478	[DAG(17:2/18:1) + H] <sup>+</sup>	LMGL02010038	605.51395	605.51465	1.1560427	4343
	623	505, 478, 579, 434	[PI(20:3) + H] <sup>+</sup>	LMGP06050021	623.31909	623.31963	0.86633	81186
MBH	635	591, 446, 464, 402	[DAG(18:4/20:5) + H] <sup>+</sup>	LMGL02010513	635.46700	635.46748	0.75535	58885
	651	462, 607, 418, 480	[DAG(17:2/22:6) + H] <sup>+</sup>	LMGL02010206	651.4983	651.49897	1.0283987	4549
	675	631, 486, 587	[PA(16:0/18:1) + H] <sup>+</sup>	LMGP10010007	675.49593	675.49634	0.6069615	40928
	846	635, 657, 675, 802, 613, 569	[TAG(17:0/17:1/17:1) + H] <sup>+</sup>	LMGL03010045	845.75927	845.7599	0.7448928	4744
	862	673, 651, 818	[PI(22:2/14:1) + H] <sup>+</sup>	LMGP06010728	861.54876	861.54796	-0.9285603	80750
	886	842, 697, 653, 675, 715, 631, 798	[TAG(17:1/17:2/20:0) + H] <sup>+</sup>	LMGL03010233	885.79057	885.79147	1.0160415	4930
	887	843, 698, 654, 676, 632, 716	[PC(21:0/22:1) + H] <sup>+</sup>	LMGP01011977	886.72593	886.72643	0.5638721	76257
	665	635, 647, 353, 325, 371, 520, 621	[PC(16:0/12:0) + H] <sup>+</sup>	LMGP01020176	664.52757	664.52733	-0.3611588	76407
FBH	761	717, 743, 572, 673, 616	[PC(16:0/18:1) + H] <sup>+</sup>	LMGP01010581	760.58505	760.58599	1.2358907	39323
	764	720, 746, 718, 575, 736, 619, 704, 601	[PG(13:0/22:1) + H] <sup>+</sup>	LMGP04010089	763.54836	763.54887	0.6679341	78914
	823	779, 634, 777, 678, 542, 735, 805	[PC(16:0/23:5) + H] <sup>+</sup>	LMGP01010656	822.60073	822.60168	1.1548738	39397

PG, Phosphoglycerol.

\*LM ID, Lipid MAPS ID

\*\*METLIN ID

## Spatial distribution of chemical markers in adult worms

Individual worms were submitted to MS/MS analysis. In Figures 5 and 6, images clearly revealed different spatial distribution of chemical markers. It was possible to distinguish some characteristic structures of the worms' anatomy, e.g. suckers, digestive and reproductive systems. Additionally, we could also visualize the gynaecophoric channel in male's body, which is located in the tegument. All worms were positioned with suckers vertically down.

*Figure 5. Adult worm images generated by MS, selected using each of the parent ions in MS/MS mode. Images were acquired as one run for each m/z. Female and male BH strain (FBH and MBH, respectively). Pos, posterior portion; Ant, anterior portion; R, reproductive system; D, digestive system; VS, ventral sucker; OS, oral sucker and GC, Gynaecophoric channel.*

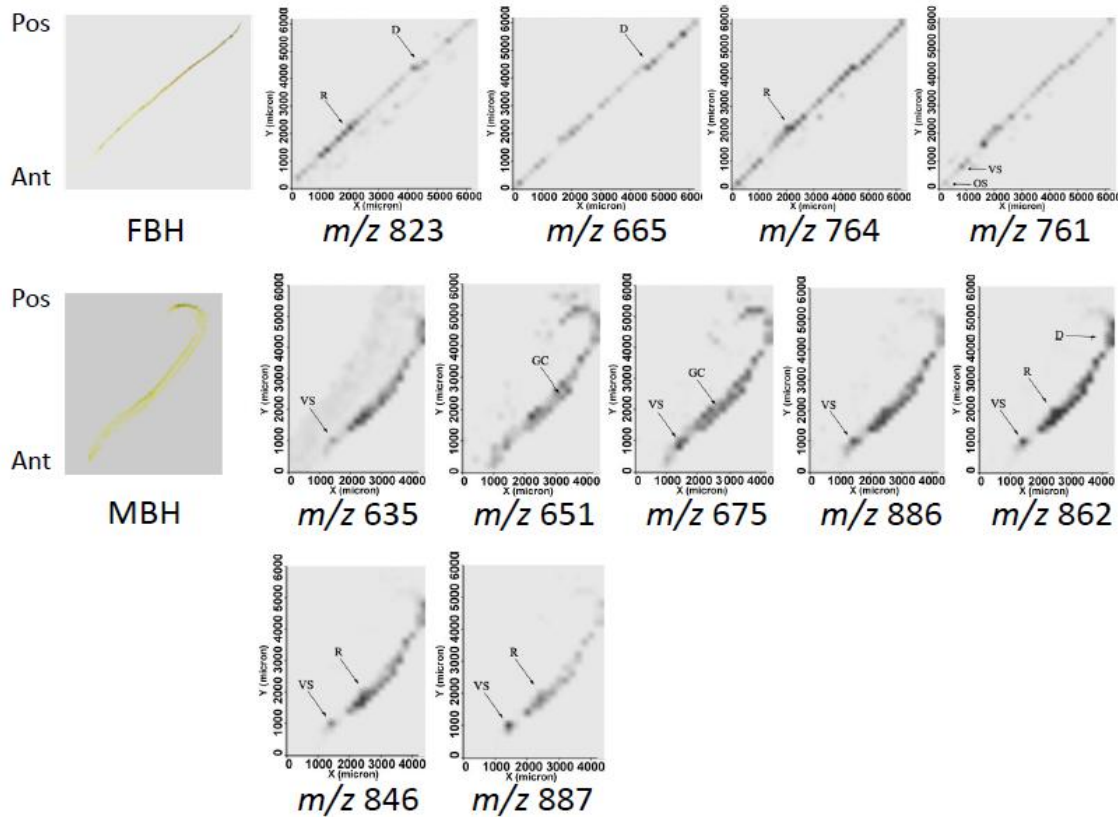
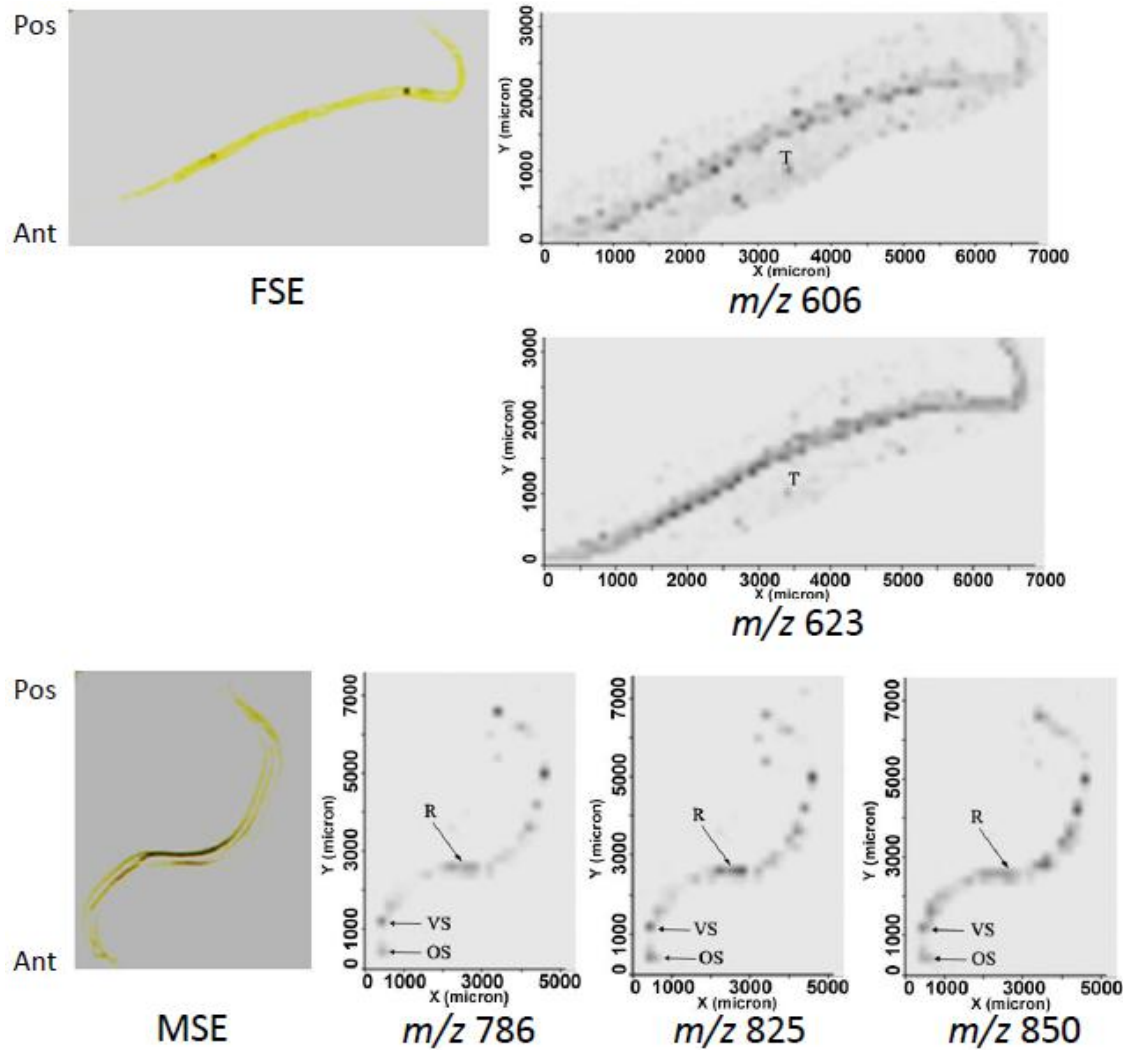


*Figure 6. Adult worm images generated by MS, selected using each of the parent ions in MS/MS mode. Images were acquired as one run for each m/z. Female and male SE strain (FSE and MSE, respectively). Pos, posterior portion; Ant, anterior portion; R, reproductive system; VS, ventral sucker and OS, oral sucker.*



## DISCUSSION

Although previous works have demonstrated *S. mansoni* worms' composition [9, 10, 23], none of them were able to differentiate them by sex and/or strains. Furthermore, most of the existing protocols for worm characterization often require sample preparation such as extraction, which does not allow inferring the spatial distribution of compounds [23]. This report demonstrates direct whole worm

analysis by MALDI-MSI that allows distinguishing different strains of *S. mansoni* based on the worm's composition. Although the parasites are not flat, preliminary tests using an optical microscope were performed in order to assess matrix homogeneity, so that no technical artifacts regarding this condition were created (data not shown). To support the sex differentiation, metabolic fingerprinting of coupled adult worms (SE strain) was performed, i.e. the total ion current was portrayed in the spectrum as well as in the molecular image. The analysis of the coupled worms has revealed the predominance of ions attributable to the male's body. This is expected, since the female is almost completely "wrapped" by the male's body (inside the gynaecophoric channel), leaving only a small part of it out. The only female body ion that appears in this spectrum was at  $m/z$  825, which was the most intense on the female SE strain (FSE) spectra. This also corroborates the fact that only lipids in the exterior of the worms' bodies are being observed; if the laser were powerful enough to pass through the worms, it would be possible to see many more signals referring to the female's body, which did not happen.

To separate the schistosomes by sex and/or strains using specific chemical markers, PCA was performed. Males and females of both strains were clearly separated with specific ions assigned for each group. The results indicate that worms of different sexes and strains are well separated in the PC1 and PC2 space, thus corroborating what was found in the fingerprint analysis.

Among the identified chemical markers, triacylglycerols (TAGs) and phosphatidylcholines (PCs) represent the major classes, as also demonstrated by Brouwwers et al. (1997b) [23]. However, this proportion changes according to the worm's sex and strain. For example, TAGs appear only in male's bodies, while

female's composition varies according to strain. Specifically, [TAG(13:0/17:2/17:2) + H]<sup>+</sup> (*m/z* 786) and [TAG(17:0/17:0/17:0) + H]<sup>+</sup> (*m/z* 850) in MSE; and [TAG(17:0/17:1/17:1) + H]<sup>+</sup> (*m/z* 846) and [TAG(17:1/17:2/20:0) + H]<sup>+</sup> (*m/z* 886) in MBH. All TAGs were located in reproductive system and suckers. The function of triacylglycerol stores in *S. mansoni* still remains unclear, since ATP cannot be generated through the  $\beta$ -oxidation of fatty acids in these organisms [24]. However, there is a hypothesis that TAG synthesis in schistosomes is used to prevent high intracellular free fatty acid concentrations [23].

In general, lipids play important roles in the schistosomes' life. Apart from constituting biological membranes, they also participate in host recognition [25], immune response modulation and evasion [26, 27], communication [28] and development [29-31]. A report with adult worms of *S. mansoni* has demonstrated that 28% of the extracted phospholipids were PCs, followed by phosphatidylethanolamines (PEs) (25%), phosphatidylserine (PS) (15%) and phosphatidylglycerol (PG) (8%) [8]. Moreover, they also observed phosphatidylinositol (PI) and phosphatidic acid (PA) in 10% of extract. Even in fewer concentrations, these phospholipids are present in schistosomes and could serve as chemical markers to some strains, such as MBH and FSE [32].

Diacylglycerol (DAG) species were also found in tegument of males and females' bodies (MBH and FSE). Presence of [DAG(17:2/22:6) + H]<sup>+</sup> (*m/z* 651) is highlighted in the GC portion of MBH worms, suggesting this compound is present only in worm's external portion. Differently, [DAG (18:4/20:5) + H]<sup>+</sup> (*m/z* 635) were located in MBH tegument and ventral sucker, while [DAG (17:2/18:1) + H]<sup>+</sup> (*m/z* 606) and [PI(20:3) + H]<sup>+</sup> (*m/z* 623) were distributed only in FSE tegument.

According to Espinoza et al. (1991) [33], DAGs are cleaved from PIs and are used in the biosynthesis of acetylcholinesterase (AChE) in *S. mansoni*. AChE is an ectoenzyme released on schistosome's surface when the worm frees itself from the membrane to which it is anchored [33].

Some phospholipids were mainly located in reproductive system and ventral sucker, such as  $[PC\ (17:0/22:4)\ + H]^+$  (*m/z* 825),  $[PI\ (22:2/14:1)\ + H]^+$  (*m/z* 862) and  $[PC\ (21:0/22:1)\ + H]^+$  (*m/z* 887) in males' bodies of both strains. It is also possible to visualize the oral sucker both in MSE and FBH. It is important to note that all chemical markers of females from the BH strain were phospholipids, and some molecules were more concentrated in digestive system, e.g.  $[PC(16:0/12:0)\ + H]^+$  (*m/z* 665) and  $[PC(16:0/23:5)\ + H]^+$  (*m/z* 823). Although functional relevance of these molecules in *S. mansoni* still remains unknown, the characterization of different strains has great potential to help understanding the role they play in virulence and even resistance to existing treatments.

## CONCLUSIONS

In summary, our results demonstrated that worms' composition depend on sex and strain. This distinction could be related to different pathogenesis, as previously described [7, 34]. Thus, characterization of adult *S. mansoni* may allow schistosomiasis control by investigation of new targets according worms' composition, molecule distribution and therefore aggressiveness of disease. For greater understanding, studies in people are required. This new trend in the study of parasite composition and distribution by mass spectrometry in combination with

metabolomic strategies has generated a new analytical platform and hence coined a new term in parasitology: *parasitomics*.

## **ACKNOWLEDGMENTS**

This work was financially supported by CAPES (Coordination for the Improvement of Higher Level -or Education- Personnel), FAPESP (São Paulo Research Foundation), CNPq and INCT (National Science and Technology Institutes).

## REFERENCES

- [1] B. Gryseels, K. Polman, J. Clerinx, L. Kestens, *The Lancet* 2006, 368, 1106.
- [2] P. Jordan, G. Webbe, *Human schistosomiasis*. 1969.
- [3] T. Quack, S. Beckmann, C. Grevelding, *Berliner und Munchener tierarztliche Wochenschrift* 2006, 119, 365.
- [4] R. N. de Oliveira, V. L. Rehder, A. S. Santos Oliveira, I. M. Junior, J. E. de Carvalho, A. L. de Ruiz, L. Jeraldo Vde, A. X. Linhares, S. M. Allegretti, *Exp Parasitol* 2012, 132, 135.
- [5] A. G. Ross, P. B. Bartley, A. C. Sleigh, G. R. Olds, Y. Li, G. M. Williams, D. P. McManus, *N Engl J Med* 2002, 346, 1212.
- [6] E. M. Martinez, R. H. Neves, R. M. F. d. Oliveira, J. R. Machado-Silva, L. Rey, *Revista da Sociedade Brasileira de Medicina Tropical* 2003, 36, 557.
- [7] L. Yoshioka, E. M. Zanotti-Magalhães, L. A. Magalhães, A. X. Linhares, *Revista da Sociedade Brasileira de Medicina Tropical* 2002, 35, 203.
- [8] B. W. Young, R. B. Podesta, *The Journal of parasitology* 1986, 72, 802.
- [9] M. Wuhrer, R. D. Dennis, M. J. Doenhoff, G. Lochnit, R. Geyer, *Glycobiology* 2000, 10, 89.
- [10] S. Frank, I. van Die, R. Geyer, *Glycobiology* 2012, 22, 676.
- [11] D. S. Cornett, M. L. Reyzer, P. Chaurand, R. M. Caprioli, *Nature Methods* 2007, 4, 828.
- [12] E. G. Solon, 2007.
- [13] C. J. Earnshaw, V. A. Carolan, D. S. Richards, M. R. Clench, *Rapid Communications in Mass Spectrometry* 2010, 24, 1665.
- [14] D. N. de Oliveira, S. de Bona Sartor, M. S. Ferreira, R. R. Catharino, *Materials* 2013, 6, 1000.
- [15] P. J. Todd, T. G. Schaaff, P. Chaurand, R. M. Caprioli, *Journal of Mass Spectrometry* 2001, 36, 355.
- [16] J. M. Wiseman, D. R. Ifa, Q. Song, R. G. Cooks, *Angewandte Chemie International Edition* 2006, 45, 7188.
- [17] P. Nemes, A. S. Woods, A. Vertes, *Analytical chemistry* 2010, 82, 982.
- [18] L. Olivier, M. A. Stirewalt, *J Parasitol* 1952, 38, 19.
- [19] S. R. Smithers, R. J. Terry, *Parasitology* 1965, 55, 695.
- [20] S. H. Xiao, J. Keiser, J. Chollet, J. Utzinger, Y. Dong, Y. Endriss, J. L. Vennerstrom, M. Tanner, *Antimicrob Agents Chemother* 2007, 51, 1440.
- [21] S. Urayama, W. Zou, K. Brooks, V. Tolstikov, *Rapid Communications in Mass Spectrometry* 2010, 24, 613.
- [22] E. Bligh, W. J. Dyer, *Canadian journal of biochemistry and physiology* 1959, 37, 911.
- [23] J. F. Brouwers, I. Smeenk, L. M. van Golde, A. G. Tielens, *Molecular and biochemical parasitology* 1997, 88, 175.
- [24] J. Barrett, *Biochemistry of parasitic helminths*, MacMillan Publishers Ltd., 1981.
- [25] A. Fusco, B. Salafsky, B. Ellenberger, L.-H. Li, *The Journal of parasitology* 1988, 253.
- [26] F. G. Abath, R. C. Werkhauser, *Parasite immunology* 1996, 18, 15.
- [27] D. J. McLaren, *Parasitology* 1984, 88, 597.

- [28] B. Fried, M. A. Haseeb, Role of lipids in *Schistosoma mansoni*, *Parasitol Today*. 1991 Aug;7(8):204; author reply 204., 1991.
- [29] T. M. Smith, T. J. Brooks, *Parasitology* 1969, 59, 293.
- [30] J. Shaw, I. Marshall, D. Erasmus, *Experimental Parasitology* 1977, 42, 14.
- [31] D. J. Hockley, D. J. McLaren, *International Journal for Parasitology* 1973, 3, 13.
- [32] J. F. Brouwers, J. J. Van Hellemond, L. M. van Golde, A. G. Tielens, *Molecular and biochemical parasitology* 1998, 96, 49.
- [33] B. Espinoza, I. Silman, R. Arnon, R. Tarrab-Hazdai, *European journal of biochemistry* 1991, 195, 863.
- [34] K. S. Warren, *Transactions of the Royal Society of Tropical Medicine and Hygiene* 1967, 61, 795.

## **CAPÍTULO II**

**Revelando alvos moleculares de Praziquantel**

**utilizando Espectrometria de Massas por**

**Imagen: uma abordagem rápida aplicada para**

***Schistosoma mansoni.***

# Revealing Praziquantel Molecular Targets using Mass Spectrometry Imaging: an Expeditious Approach Applied for *Schistosoma mansoni*.

Mônica Siqueira Ferreira<sup>1§</sup>, Rosimeire Nunes de Oliveira<sup>2§</sup>, Diogo Noin de Oliveira<sup>1</sup>, Silmara Marques Allegretti<sup>2\*</sup>, Rodrigo Ramos Catharino<sup>1\*</sup>

**1** Innovare Biomarkers Laboratory, Medicine and Experimental Surgery Nucleus, University of Campinas, Campinas, São Paulo, Brazil. **2** Biology Institute, Animal Biology Department, University of Campinas, Campinas, São Paulo, Brazil.

<sup>§</sup>These authors contributed equally to this work.

\*Corresponding author. Tel.: +55 19 3521 9138.

E-mail address: [rrc@fcm.unicamp.br](mailto:rrc@fcm.unicamp.br) (R.R. Catharino) and [sallegre@unicamp.br](mailto:sallegre@unicamp.br) (S.M. Allegretti).

## ABSTRACT

Finding specific molecular targets of Praziquantel (PZQ) in the treatment of schistosomiasis is still a challenging task. Apart from helping unravel the drug's mechanism of action, it may also lead the way towards the development of new and more effective molecules. We hereby present a mass spectrometry imaging-based approach that helps identifying and characterizing lipids directly involved in the biochemical pathways of the BH strain of *Schistosoma mansoni*, as well as differentiating the molecular response that each worm sex presents *in vivo*. Results have proven to be in accordance with previous studies and have further demonstrated significant differences, especially in the phospholipid content of PZQ-exposed adult worms when compared to the unexposed (control) group. Interestingly, female worms exposed to PZQ presented phosphatidylethanolamine associated to ceramide (PE-Cer) as chemical marker. PE-Cer is in sphingolipid category and can be inserted in cell death pathway. While male worms treated with PZQ presented only phosphoinositol species identified as adducts of sodium ( $[M+Na]^+$ ) and potassium ( $[M+K]^+$ ) as chemical markers. This suggests the

possibility that the (Na<sup>+</sup> K<sup>+</sup>)-ATPase is being impaired due to PZQ exposure, meaning that this enzyme can be an important target to new drugs development to schistosomiasis treatment.

## AUTHOR SUMMARY

Schistosomiasis is an infection that has the largest geographic distribution, affecting thousands of people in Africa, Middle East, South America and the Caribbean. Among the five species, only *Schistosoma mansoni* is found in Brazil. Besides the high incidence and prevalence of schistosomiasis, treatment is based only on a single drug: Praziquantel (PZQ). However, it is not 100% effective on adult *S. mansoni*. Although several studies have demonstrated PZQ mechanism of action, much is still unknown. To better understand some of these mechanisms, chemical markers can be identified, suggesting possible biological pathways. In this study, we demonstrated that male and female worms possibly present different metabolic pathways in response to PZQ. Furthermore, knowing the location of these responsive chemical markers in the worm's body could lead to important target-molecules that will assist in future drug development for schistosomiasis.

## 1. INTRODUCTION

Praziquantel (PZQ) is the most common drug prescribed for all forms of schistosomiasis, since it is equally effective against *Schistosoma mansoni*, *S. japonicum*, *S. mekongi*, *S. intercalatum*, and *S. haematobium* [1, 2]. However, it is not 100% effective on adult *S. mansoni*: generally, a cure rate of 60% or greater is obtained with PZQ treatment [3]. Additionally, it is less effective against the immature stages of the parasite [4-6].

PZQ mechanism of action has been studied for several years [7-10]. Some physiological and morphological aspects have been unraveled for a relatively long time, such as rapid  $\text{Ca}^{2+}$  ions uptake [11] and vacuolation and blebbing near and on the surface [12]. In male worms, in addition to its effects on  $\text{Ca}^{2+}$  concentration, PZQ stimulates  $\text{Na}^+$  influx in a non-ionophore mechanism [11]. Furthermore, PZQ induces modifications in membrane fluidity as well as in phospholipid composition, producing alterations in its permeability to ions or resulting in indirect effects on membrane receptors and channels [13, 14]. However, some mechanisms still remain unknown; for example, the pathway of  $\text{Ca}^{2+}$  homeostasis disruption by PZQ in adult schistosomes [15, 16] and the mechanism of the PZQ binding to its molecular targets [17, 18] are still to be unraveled.

To better understand some of these mechanisms, modern analytical approaches, e.g. chromatographic techniques combined with mass spectrometry (MS), have been employed for chemical characterization of adult schistosomes and PZQ metabolites in the host [19-21]. More recently, matrix-assisted laser desorption/ionization MS (MALDI-MS) has been applied as the main analytical tool [22]. Approaches using MS Imaging (MALDI-MSI) [23], were developed to identify the spatial distribution of compounds in any physical sample, such as tissue sections [24], single cell [25], drug tablets [26] and cosmetic products [27]. Moreover, MALDI-MSI was applied, for the first time, in *S. mansoni* adult worms to demonstrate different chemical markers according schistosome sex and strain [28]. This study allowed us to localize each identified compound in the worm's body. Since schistosomes show stage- and sex-dependent differences in susceptibility to

PZQ [6], information on possible targets and pathways of the drug could be clarified by chemical markers localization.

Based on this, the present work has employed the metabolomic platform to characterize both sexes of *S. mansoni* adult worms treated with PZQ. This report identifies the spatial distribution of chemical markers using MALDI-MSI technology, aiding the search for understanding of possible targets and pathways of this antischistosomal drug.

## **2. MATERIAL AND METHODS**

### *2.1. Mice infection by S. mansoni*

Balb/C albino female mice with 30 days-old, weighing 18-20g, were individually infected with ~70 *S. mansoni* cercariae of the BH strain (from Belo Horizonte, MG, Brazil). At this stage, the utilized procedure was caudal immersion for 2 hours, with light exposure and controlled temperature of 28°C [29]. After 45 days of the infection, animals were divided in two groups (n=5/group): (i) treated with PZQ (Merck, Darmstadt, Germany) and (ii) negative control. The first group received a single oral dose of 40 mg/kg of PZQ, using esophageal tubing. Control group received PBS 1x solution. PZQ concentration used in the present study is considered equivalent to the one utilized in humans, as adopted by the schistosomiasis treatment and control programs in Brazil. This study was carried out in strict accordance with the recommendations in the Guide for the Care and Use of Laboratory Animals. The protocol was approved by the International Ethics Commission for the Use of Animals (CEUA/ICCLAs, protocol nº 2170-1).

## *2.2. Recovery of *S. mansoni* worms*

Two weeks after treatment, mice were submitted to cervical dislocation. *S. mansoni* adult worms were recovered by perfusion of the hepatic portal system and mesenteric veins [30]. All worms were washed in saline solution followed by H<sub>2</sub>O milliQ.

## *2.3. MALDI-MSI analysis*

All adult *S. mansoni* worms were deposited in a thin-layer chromatography (TLC) plate (Merck, Darmstadt, Germany). Matrix coating was performed using a commercial airbrush, spraying α-cyano-4-hydroxycinnamic acid (Sigma-Aldrich, Pennsylvania, USA) (10 mg/mL in 1:1 Acetonitrile/Methanol solution). Images and mass spectra were acquired in a MALDI-LTQ-XL instrument equipped with imaging feature (Thermo Scientific, California, USA). The instrument uses a Nd:YAG laser as ionization source and a quadrupole-ion-trap analyzing system. All data were acquired in the positive ion mode. For image acquisition, a 50 μm raster width was selected. Fragmentation data (MS/MS) were acquired by setting the collision-induced normalized energy to 40. Helium was used as the collision gas. Each ion was fragmented in triplicates. All imaging data were then processed using ImageQuest software v.1.0.1 (Thermo Scientific, California, USA).

## *2.4. Statistical analysis and biomarker identification*

Mass and intensity values for each spectrum were included in the Principal Component Analysis (PCA), which has been performed using Unscrambler v.9.7 (CAMO Software, Trondheim, Norway). MS/MS reactions were performed with

each potential biomarker identified by PCA. Lipid MAPS online database (University of California, San Diego, CA – [www.lipidmaps.org](http://www.lipidmaps.org)) and METLIN (Scripps Center for Metabolomics, La Jolla, CA) were consulted to help guiding the choice for potential lipid markers. Their structures were later proposed using Mass Frontier software v.6.0 (Thermo Scientific, California, USA) [31].

### *2.5. High resolution ESI-MS analysis.*

To confirm the chemical markers identifications, males and females treated or not with PZQ were submitted to a Bligh-Dyer extraction [32]. Lipid extracts were resuspended in 50 µL of H<sub>2</sub>O milliQ and 10 µL of the latter was diluted in 990 µL of methanol and 0.1% formic acid. Data acquisition was performed in a LTQ-XL Orbitrap Discovery instrument (Thermo Scientific, Bremen, Germany) in the positive ion mode and at the *m/z* range of 600-2000 for complex lipid identification. Structural propositions were performed using high resolution as the main parameter. Mass accuracy was calculated and expressed in terms of ppm shifts.

## **3. RESULTS**

### *3.1. Metabolic fingerprint of adult worms*

Male and female adult worms, treated or not with PZQ, were subjected to MALDI-MSI analysis, as described in methods. All of them presented clear differences in their spectra when compared to each other (Figure 7).

### *3.2. Statistical analysis and biomarkers identification*

Statistical analysis was performed by the comparison between male and female, treated or not with PZQ. As shown in Figure 8, worm control groups (MCT and FCT) were clearly separated of worms submitted to PZQ treatment with an accuracy of 99%. The identified ions compose the final model of optimized PCA.

For chemical marker identification, ion fragmentation reactions (MS/MS) were performed and then compared to characteristic fragmenting patterns either predicted by software or found in databases, as described in the “Materials and Methods” section. High-resolution Fourier transform MS (HR-FTMS) was also utilized at this stage, with experimental masses compared to theoretical found at METLIN database. Table 2 presents chemical markers identified in each adult worm, as well as the precursor ion fragmentation and the mass errors for each signal observed in HR-FTMS, measured in ppm (with all results presenting a deviation of less than 2 ppm).

*Figure 7. Representative fingerprinting spectra of *S. mansoni* adult worms. (A) Female control (FCT). (B) Male control (MCT). (C) Female treated with PZQ (FPZQ). (D) Male treated with PZQ (MPZQ). Positive ion mode.*

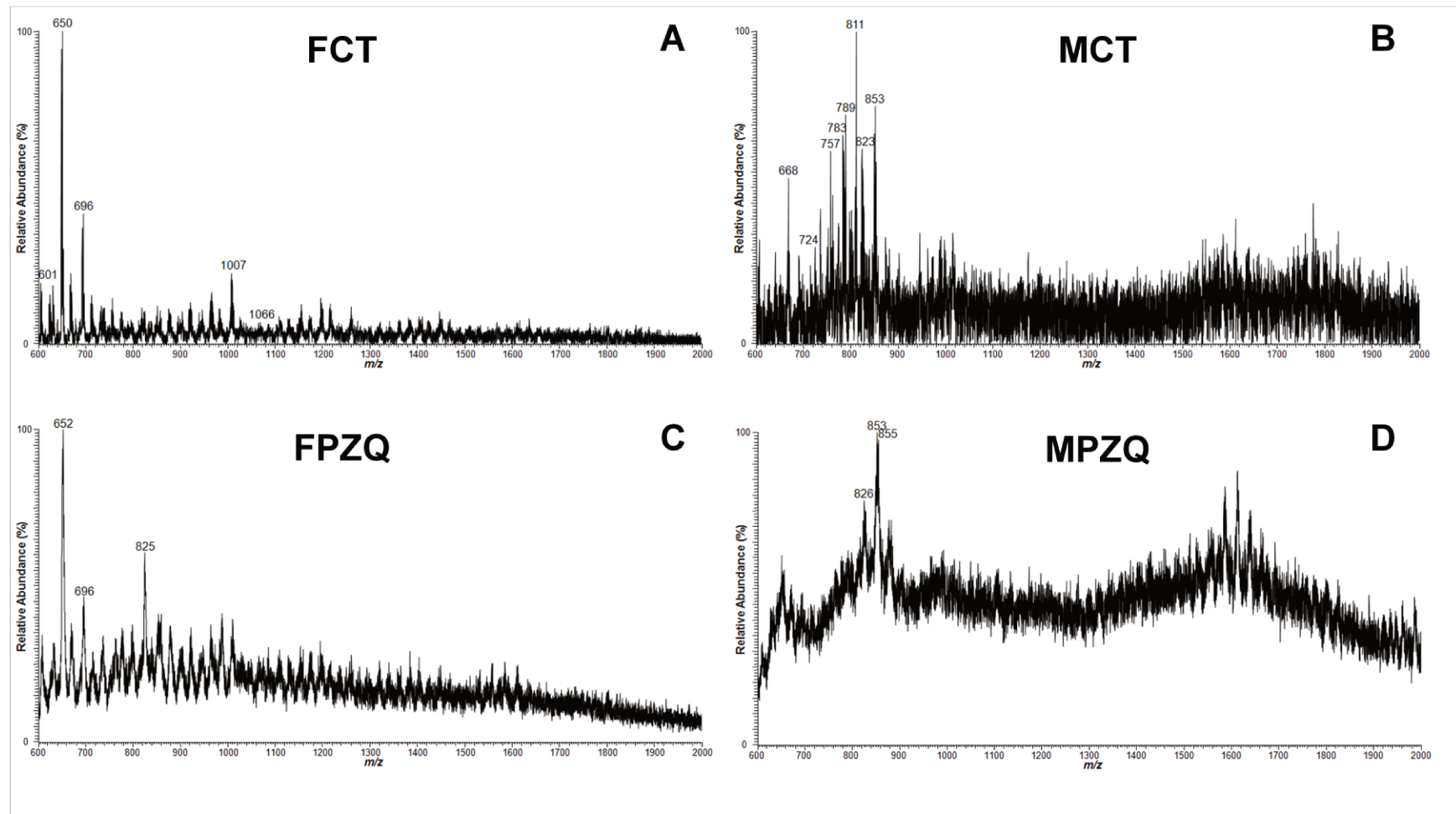
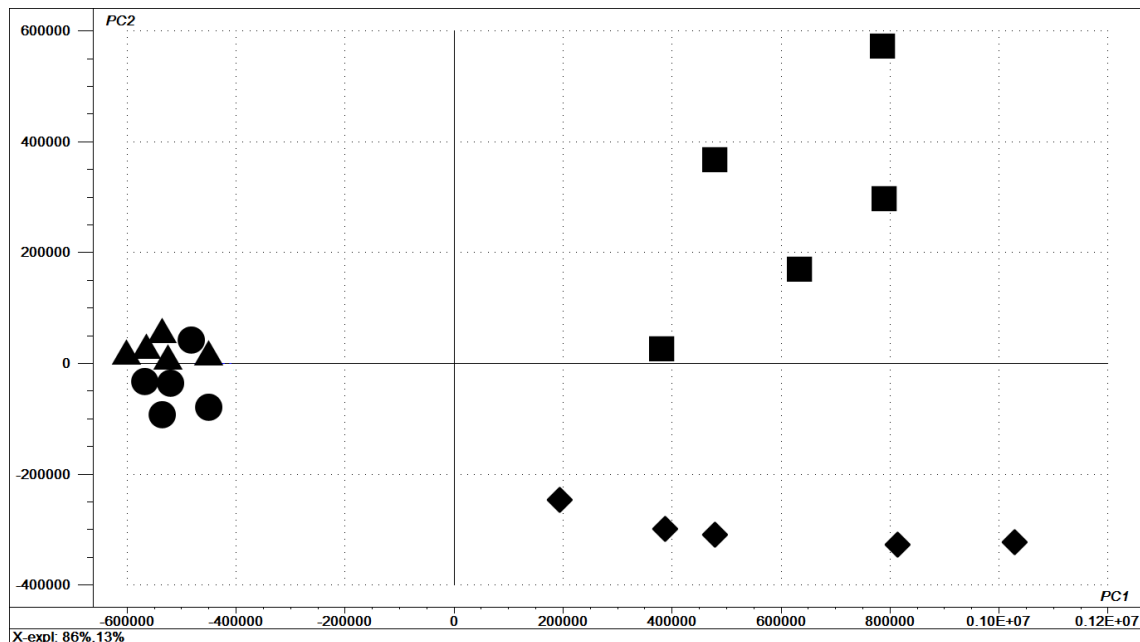


*Figure 8. Principal Component Analysis (PCA) of *S. mansoni* adult worms. Ion biomarkers of each group separated by PCA ( $n=5/\text{group}$ ). The explained variances (X-expl) are shown on inferior part of the figure. ▲, male negative control (MCT). ●, female negative control (FCT). ♦, male treated with PZQ (MPZQ). ■, female treated with PZQ (FPZQ).*



### 3.3. Spatial distribution of biomarkers in adult worms

Individual worms were submitted to MS/MS analysis. In Figures 9-12, images clearly revealed different spatial distribution of chemical markers. It was possible to distinguish some characteristic anatomical structures of the worms, e.g. suckers, gut, reproductive systems, and tegument.

*Table 2. Lipid chemical markers identified via MALDI-MSI of *S. mansoni* adult worms (positive ion mode).*

Adult worms	Parental ion ( <i>m/z</i> )	Product ions ( <i>m/z</i> )	Molecule	LM ID*	Theoretical Mass	Experimental Mass	Error (ppm)	MID**
FCT / MCT	601	557, 583	[DG(17:2/18:3/0:0)+H] <sup>+</sup>	LMGL02010051	601,4826	601,4818	-1,330046788	4357
	617	558, 457, 413	[PA(12:0/18:2)+H] <sup>+</sup>	LMGP10010051	617,4177	617,417	-1,133754345	81217
	619	448, 430, 560	[PA(13:0/17:1)+H] <sup>+</sup>	LMGP10010072	619,4333	619,433	-0,484313646	81238
	620	475, 502, 576	[PE(12:0/15:1)+H] <sup>+</sup>	LMGP02010361	620,4286	620,4291	0,805894506	76596
	724	680, 606, 579, 706	[PC(12:0/20:5)+H] <sup>+</sup>	LMGP01011333	724,4912	724,4899	-1,79436272	75613
	726	682, 581, 710	[PC(14:0/18:4)+H] <sup>+</sup>	LMGP01010499	726,5068	726,506	-1,101159686	59327
FPZQ	651	584, 462, 480	[PG(12:0/15:1)+H] <sup>+</sup>	LMGP04010048	651,4232	651,424	1,228080302	78873
	652	463, 585, 608	[PS(14:0/12:0)+H] <sup>+</sup>	LMGP03010931	652,4184	652,4175	-1,379482859	78595
	649	460, 605, 582	[PE-Cer(14:1/18:0)+H] <sup>+</sup>	LMSP03020059	649,4915	649,4905	-1,539666031	103098
MPZQ	853	809, 708, 664	[PI(12:0/22:4)+Na] <sup>+</sup>	LMGP06010035	853,4837	853,4833	-0,468667416	80057
	855	666, 811, 684	[PI(13:0/20:4)+K] <sup>+</sup>	LMGP06010054	855,442	855,4431	1,285884958	80076
	827	768, 682, 783	[PI(12:0/20:3)+Na] <sup>+</sup>	LMGP06010029	827,4681	827,4688	0,845954061	80051

DG, diacylglycerol; PA, phosphatidic acid; PE, phosphoethanolamine; PC, phosphatidylcholine; PG, phosphoglycerol; PS, phosphatidylserine; PI, phosphoinositol; Cer, ceramide.

Identification is based on MS/MS data, exact mass of each compound and Lipid Maps and METLIN databases.

\* LM ID, Lipid MAPS ID.

\*\*MID, METLIN ID.

*Figure 9. Male control adult worm images generated by MS/MS. Pos, Posterior portion. Ant, Anterior portion. T, Tegument. OS, Oral sucker. G, Gut.*

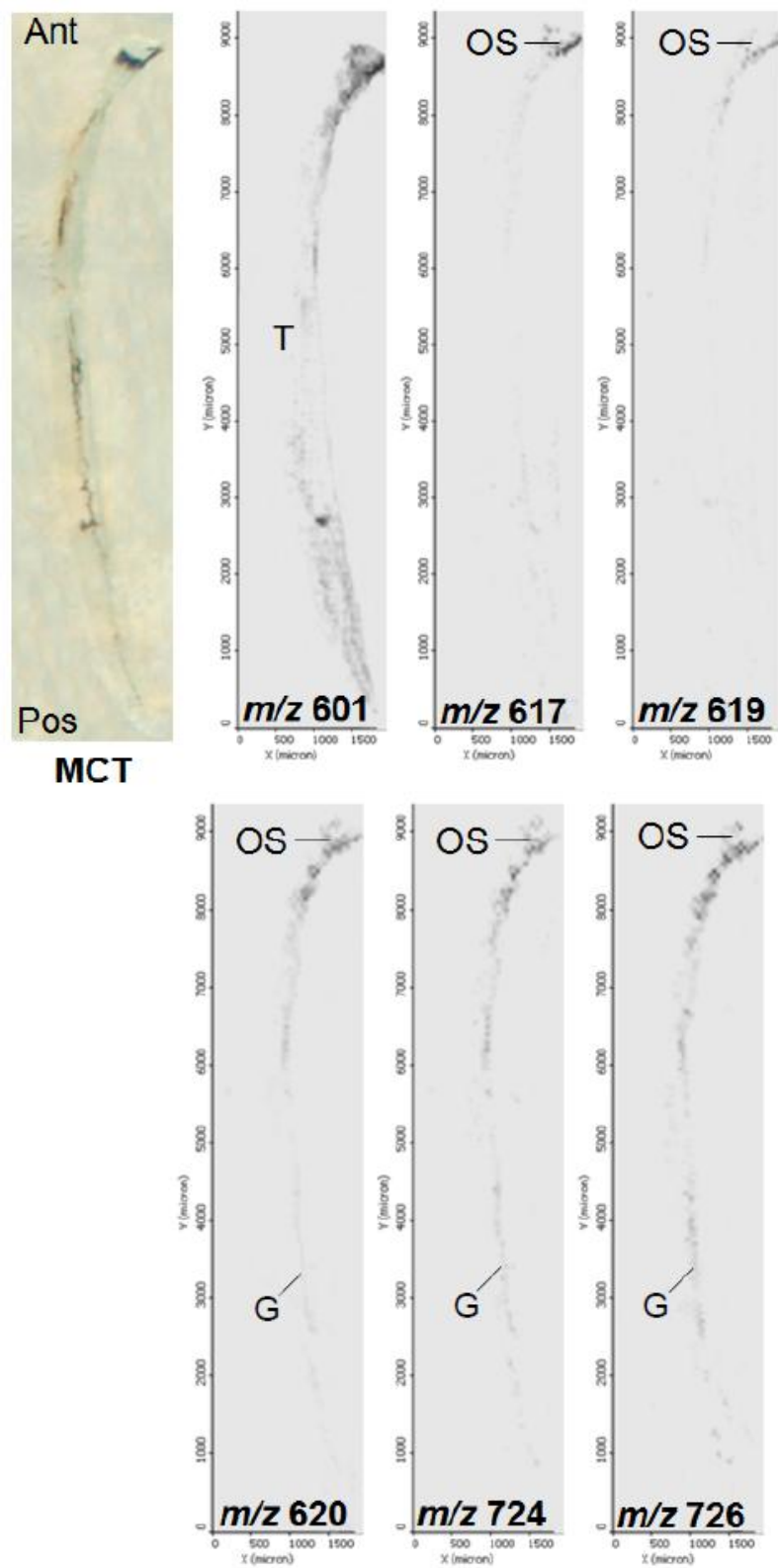


*Figure 10. Female control adult worm images generated by MS/MS. Pos, Posterior portion. Ant, Anterior portion. R, Reproductive system. G, Gut. T, Tegument.*

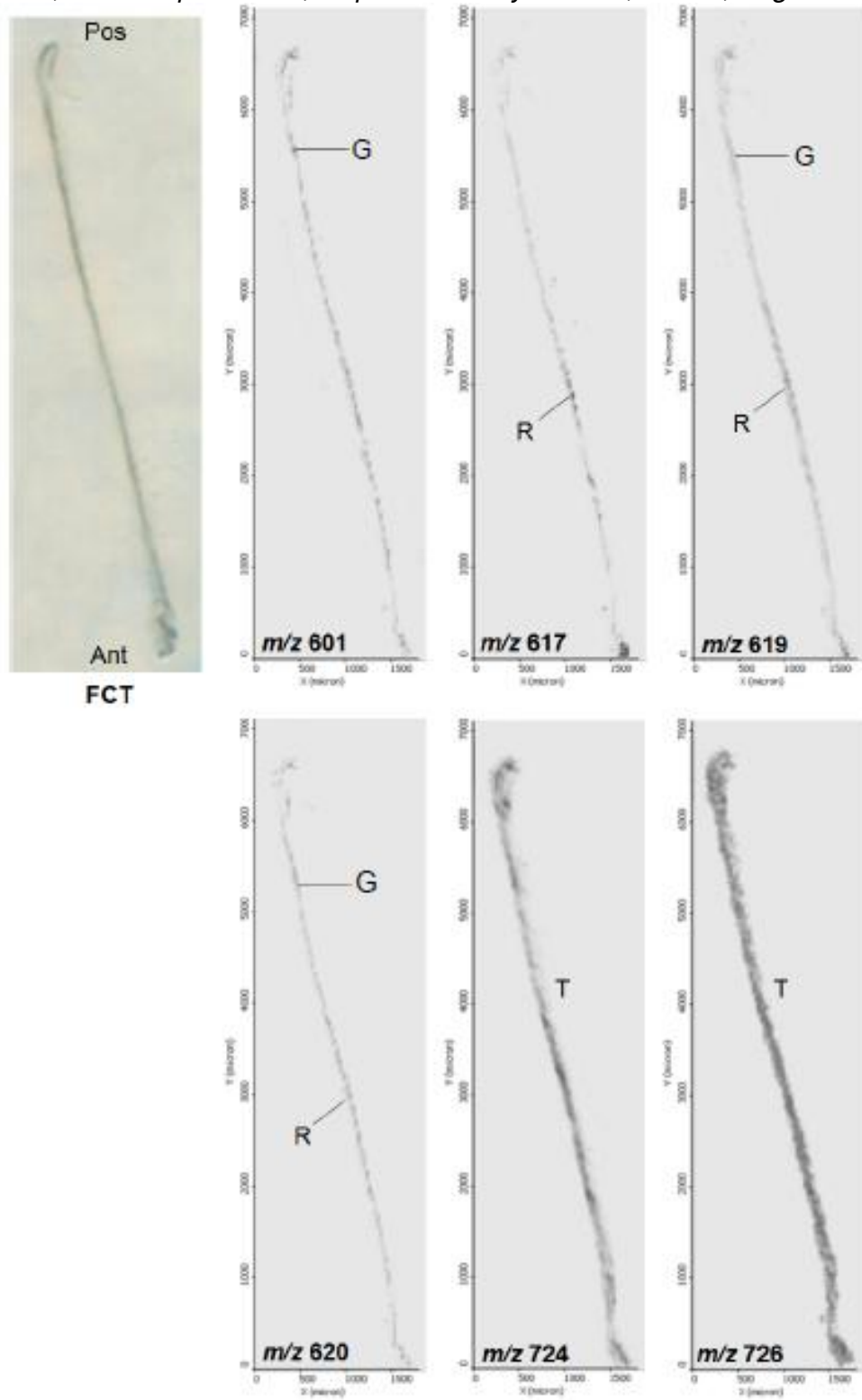


*Figure 11. Male adult worm treated with PZQ images generated by MS/MS. Pos, Posterior portion. Ant, Anterior portion. R, Reproductive system. OS, Oral sucker. G, Gut.*

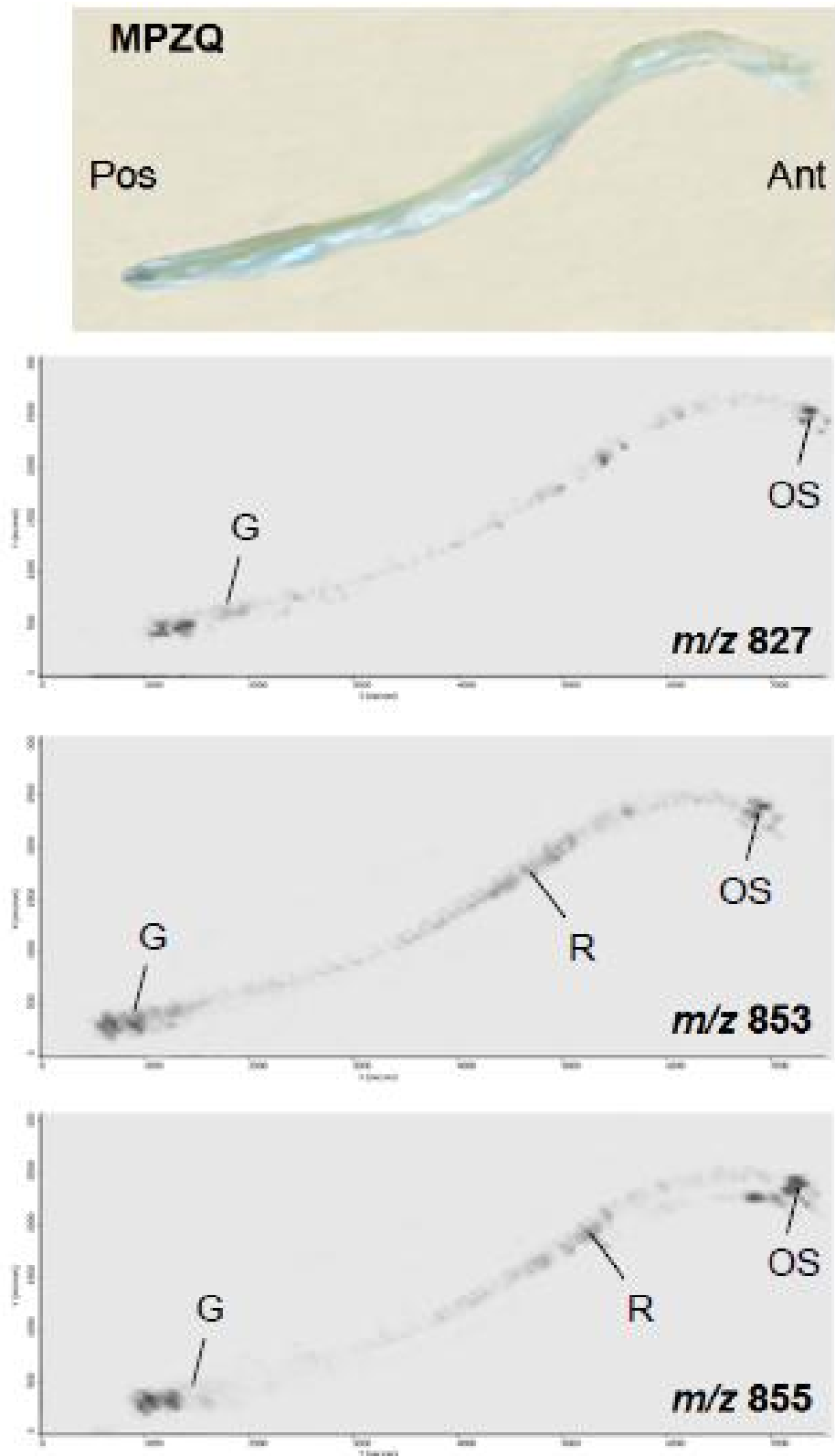
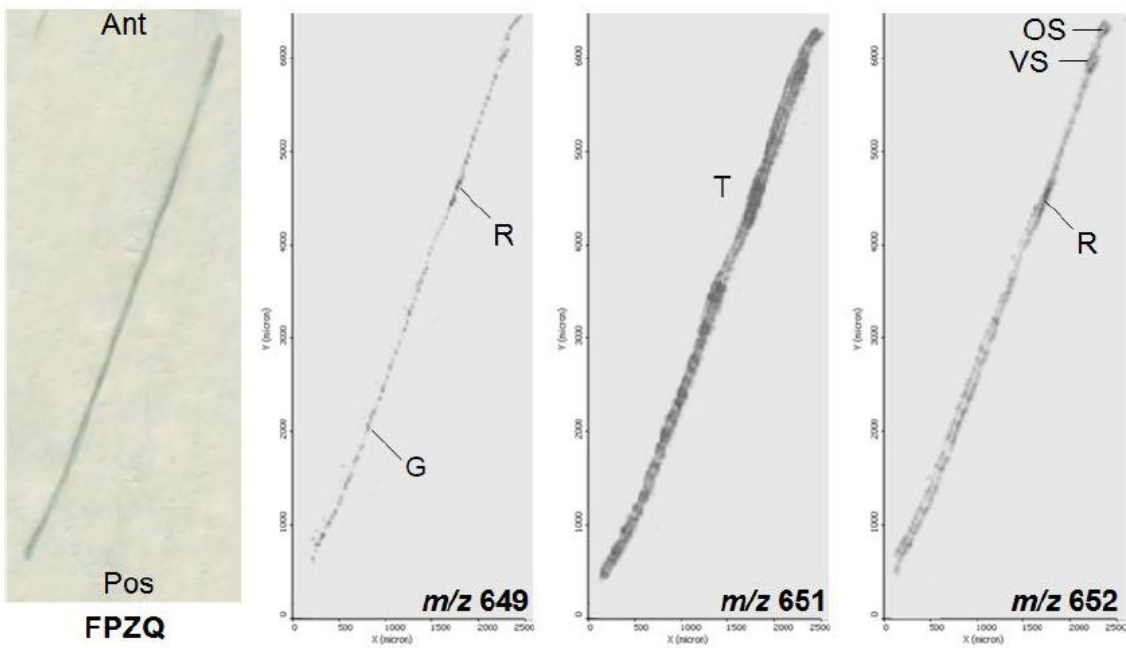


*Figure 12. Female adult worm treated with PZQ images generated by MS/MS. Pos, Posterior portion. Ant, Anterior portion. R, Reproductive system. T, Tegument. G, Gut. OS, Oral sucker. VS, Ventral sucker.*



#### 4. DISCUSSION

Recently, a study performed in our laboratory has already demonstrated the spatial distribution of lipids in adult worms of two Brazilian strains of *S. mansoni* (*in vitro*): BH and SE [28] using MALDI-MSI and the lipidomics approach. In the present report, we applied the same tools to identify metabolic alterations caused by PZQ treatment in BH strain *S. mansoni* (*in vivo*). Although it is the same strain, parasites obtained *in vivo* could present different lipid profile when compared to *in vitro* results, since schistosomes use compounds from the host in lipid synthesis [33]. Interestingly, fingerprint of *in vivo* control adult worms, both male and female, presented a similar spectrum profile when compared to *in vitro* [28]. This result

demonstrates the precision of the method to identify and differentiate schistosomes by sex (Figure 7, A and B).

Furthermore, besides tegumental damages, PZQ has significantly changed the metabolic profile of both sex of *S. mansoni* (Figure 7, C and D). This modification was enough to segregate almost all groups in PCA analysis, except control male and female groups (Figure 7). Probably, most compounds derived from the host, providing very close similarities between both sexes. However, PZQ reaches differentially each one [6], which could explain the MPZQ and FPZQ segregation in PCA.

Among the identified chemical markers, phospholipids (PLs) represent the major class, as also related by Young and Podesta (1982) [34]. In general, lipids play important roles in the lives of schistosomes. Apart from constituting biological membranes, they also participate in host recognition [35], immune response modulation and evasion [36, 37], communication [38] and development [39-41].

Among PL classes, phosphatidylcholines (PCs), phosphoethanolamines (PEs) and phosphatidic acids (PAs) were found in control groups. Interestingly, the same chemical markers presented distinct spatial location in MCT and FCT. For example,  $[PA(12:0/18:2)+H]^+$  (*m/z* 617) and  $[PA(13:0/17:1)+H]^+$  (*m/z* 619) were located in the oral sucker in males, and in the reproductive system and gut of female worms. However, PA role in *S. mansoni* is yet unknown. The same occurs with  $[PC(12:0/20:5)+H]^+$  (*m/z* 724) and  $[PC(14:0/18:4)+H]^+$  (*m/z* 726), that were present in the oral sucker and gut of MCT, and in the tegument of FCT. Although functional role of these molecules in *S. mansoni* remains unknown, some studies already demonstrated that PCs are the most abundant PL class present in *S.*

*mansi* [34, 42]. Furthermore, according Brouwers et al. (1998) [42], PCs were presented in bulk in schistosomes tegument, corroborating our result obtained in FCT. Moreover,  $[PE(12:0/15:1)+H]^+$  (*m/z* 620) were located in the reproductive system and gut of females, and in the oral sucker and gut of males. Diacylglycerol  $[DG(17:2/18:3/0:0)+H]^+$  (*m/z* 601) was present in gut and tegument, respectively, of females and males bodies of the control group. This compound class was already found in tegument of adult BH strain schistosomes [28]. Furthermore, a previous study suggests that DGs are cleaved from phosphoinositol (PI) to be used in the biosynthesis of acetylcholinesterase (AChE) in *S. mansoni*. AChE is an ectoenzyme that is released on the surface of the schistosomes when the worm frees itself from the wall or organ to which it is anchored [43].

When female worms were treated with PZQ, there has been a notable change in its chemical markers: phosphoglycerol  $[PG(12:0/15:1)+H]^+$  (*m/z* 651), phosphatidylserine  $[PS(14:0/12:0)+H]^+$  (*m/z* 652) and PE coupled with ceramide  $[PE-Cer(14:1/18:0)+H]^+$  (*m/z* 649). All of them were located in different regions of the worm body. For example, PG was located in tegument, while PS presented itself more concentrated in oral and ventral suckers and reproductive system. On the other hand, PE-Cer was concentrated in gut and reproductive system. The latter is inserted in sphingolipid category and may be produced in microsomes of rat liver and plasma membrane and internalized by schistosomes, since they do not have a *de novo* synthesis pathway [44]. However, other studies demonstrated that this sphingolipids can be synthesized by *S. mansoni* females via sphingomyelinase activity, and plays a second messenger role [45-47]. This role has been established in several cell types [45, 48-50], being implicated in cell

death and differentiation. Sometimes, this second messenger role is activated in response to external stimuli, such as TNF- $\alpha$ , IFN- $\gamma$  and vitamin D3 [48, 49, 51-53]. TNF- $\alpha$ , in turn, is believed to play a preventive role for cases of superinfections [54-56]. However, PZQ also stimulates TNF- $\alpha$  expression in animals [57]. Thus, we suggest that PZQ may activate sphingolipid production in female adult worms and, more specifically, PE-Cer can also be internalized from the host production; more experiments are, however, required to prove this hypothesis, likewise to understand this chemical marker location.

Similar to females, male worms also presented different lipid profile with PZQ treatment. Three phosphoinositol (PI) derivatives were found:  $[PI(12:0/22:4)+Na]^+$  ( $m/z$  853),  $[PI(13:0/20:4)+K]^+$  ( $m/z$  855) and  $[PI(12:0/20:3)+Na]^+$  ( $m/z$  827). All of them were placed in the same spatial location in the worm's body: oral sucker, gut and reproductive system. It is also important to note that all chemical markers were identified as sodium ( $Na^+$ ) or potassium ( $K^+$ ) adducts. This information could be supported by Pax et al. (1978) [11], demonstrating that PZQ stimulates influx of  $Na^+$  in *S. mansoni* male adult worms. On the other hand, some reports related that PZQ could induce modification in membrane phospholipids, causing fluidity, which may produce alterations in permeability to ions or result in indirect effects on membrane receptors and channels [13, 14]. Moreover, Cunha and Noël (1997) [58] have described that PZQ have no effect on schistosome ( $Na^+ K^+$ )-ATPase. However, all of the previous tests were performed only in the tegument of the worm [58]. In contrast, a recent study using gene expression assay of male *S. japonicum* demonstrated that adult worms exposed to PZQ had up-regulated the sodium/potassium-transporting ATPase

gene [59]. Since chemical markers of MPZQ were located in internal structures of anatomical male worms, and all of PIs species were related with  $\text{Na}^+$  and  $\text{K}^+$ , we could suggest that tegument is not the only target involved in the worm death by PZQ.

In summary, our results suggest that male and female worms present different pathways in response to PZQ, since chemical markers were distinct according sex when treated with the drug. It could be related to the resistance level of each schistosome sex, as also demonstrated by Pica-Mattoccia and Cioli (2004) [6]. In female worms, PZQ could induct death cell by sphingomyelinase activity. Furthermore, our results indicated that possibly  $(\text{Na}^+ \text{ K}^+)$ -ATPase, in male worms, can have its activity compromised when adult worms are exposed to PZQ, making this enzyme an important target to new drugs development to schistosomiasis treatment.

## REFERENCES

1. Webbe G, James C (1977) A comparison of the susceptibility to praziquantel of *Schistosoma haematobium*, *S. japonicum*, *S. mansoni*, *S. intercalatum* and *S. mattheei* in hamsters. Zeitschrift für Parasitenkunde 52: 169-177.
2. Fenwick A, Savioli L, Engels D, Robert Bergquist N, Todd MH (2003) Drugs for the control of parasitic diseases: current status and development in schistosomiasis. Trends in parasitology 19: 509-515.
3. Danso-Appiah A, Utzinger J, Liu J, Olliaro P (2008) Drugs for treating urinary schistosomiasis. Cochrane Database Syst Rev 3.
4. Sabah A, Fletcher C, Webbe G, Doenhoff M (1986) < i> Schistosoma mansoni:</i> Chemotherapy of infections of different ages. Experimental parasitology 61: 294-303.
5. Gönnert R, Andrews P (1977) Praziquantel, a new broad-spectrum antischistosomal agent. Zeitschrift für Parasitenkunde 52: 129-150.
6. Pica-Mattoccia L, Cioli D (2004) Sex-and stage-related sensitivity of< i> Schistosoma mansoni</i> to in vivo and in vitro praziquantel treatment. International journal for parasitology 34: 527-533.
7. Doenhoff MJ, Cioli D, Utzinger J (2008) Praziquantel: mechanisms of action, resistance and new derivatives for schistosomiasis. Current opinion in infectious diseases 21: 659-667.
8. LoVerde PT, Hirai H, Merrick JM, Lee NH, El-Sayed N (2004) < i> Schistosoma mansoni</i> genome project: an update. Parasitology International 53: 183-192.
9. Hu W, Brindley PJ, McManus DP, Feng Z, Han Z-G (2004) Schistosome transcriptomes: new insights into the parasite and schistosomiasis. Trends in Molecular Medicine 10: 217-225.
10. Andrews P (1985) Praziquantel: mechanisms of anti-schistosomal activity. Pharmacology & therapeutics 29: 129-156.
11. Pax R, Bennett J, Fetterer R (1978) A benzodiazepine derivative and praziquantel: effects on musculature of *Schistosoma mansoni* and *Schistosoma japonicum*. Naunyn-Schmiedeberg's archives of pharmacology 304: 309-315.
12. Becker B, Mehlhorn H, Andrews P, Thomas H, Eckert J (1980) Light and electron microscopic studies on the effect of praziquantel on *Schistosoma mansoni*, *Dicrocoelium dendriticum*, and *Fasciola hepatica* (Trematoda) in vitro. Zeitschrift für Parasitenkunde 63: 113-128.
13. Harder A, Goossens J, Andrews P (1988) Influence of praziquantel and Ca<sup>2+</sup> on the bilayer-isotropic-hexagonal transition of model membranes. Molecular and biochemical parasitology 29: 55-59.
14. Lima S, Vieira L, Harder A, Kusel J (1994) Effects of culture and praziquantel on membrane fluidity parameters of adult *Schistosoma mansoni*. PARASITOLOGY-CAMBRIDGE- 109: 57-57.
15. Redman C, Robertson A, Fallon P, Modha J, Kusel J, et al. (1996) Praziquantel: an urgent and exciting challenge. Parasitology Today 12: 14-20.

16. Day T, Bennett J, Pax R (1992) Praziquantel: the enigmatic antiparasitic. *Parasitology Today* 8: 342-344.
17. Troiani AR, Pica-Mattoccia L, Valle C, Cioli D, Mignogna G, et al. (2007) Is actin the praziquantel receptor? *International journal of antimicrobial agents* 30: 280-281.
18. Tallima H, El Ridi R (2007) Praziquantel binds *< i> Schistosoma mansoni</i>* adult worm actin. *International journal of antimicrobial agents* 29: 570-575.
19. Meier H, Blaschke G (2000) Capillary electrophoresis-mass spectrometry, liquid chromatography-mass spectrometry and nanoelectrospray-mass spectrometry of praziquantel metabolites. *Journal of Chromatography B: Biomedical Sciences and Applications* 748: 221-231.
20. Meier H, Blaschke G (2001) Investigation of praziquantel metabolism in isolated rat hepatocytes. *Journal of pharmaceutical and biomedical analysis* 26: 409-415.
21. van Balkom BW, van Gestel RA, Brouwers JF, Krijgsveld J, Tielens AG, et al. (2005) Mass Spectrometric Analysis of the *Schistosoma m ansoni* Tegumental Sub-proteome. *Journal of proteome research* 4: 958-966.
22. Frank S, van Die I, Geyer R (2012) Structural characterization of *Schistosoma mansoni* adult worm glycosphingolipids reveals pronounced differences with those of cercariae. *Glycobiology* 22: 676-695.
23. Cornett DS, Reyzer ML, Chaurand P, Caprioli RM (2007) MALDI imaging mass spectrometry: molecular snapshots of biochemical systems. *Nature Methods* 4: 828-833.
24. Solon EG (2007) Autoradiography: high-resolution molecular imaging in pharmaceutical discovery and development. *Expert Opin Drug Discov* 2: 503-514.
25. Ferreira MS, de Oliveira DN, Gonçalves RF, Catharino RR (2014) Lipid characterization of embryo zones by silica plate laser desorption ionization mass spectrometry imaging (SP-LDI-MSI). *Analytica Chimica Acta* 807: 96-102.
26. Rodrigues LR, Oliveira DND, Ferreira MS, Catharino RR (2014) In Situ Assessment of Atorvastatin impurity using MALDI Mass Spectrometry Imaging (MALDI-MSI). *Analytica Chimica Acta* In press.
27. de Oliveira DN, de Bona Sartor S, Ferreira MS, Catharino RR (2013) Cosmetic Analysis Using Matrix-Assisted Laser Desorption/Ionization Mass Spectrometry Imaging (MALDI-MSI). *Materials* 6: 1000-1010.
28. Ferreira MS, Oliveira DN, Oliveira RN, Allegretti SM, Vercesi AE, et al. (2014) Mass spectrometry imaging: a new vision in differentiating *Schistosoma mansoni* strains. *Journal of Mass Spectrometry* 49: 86-92.
29. Olivier L, Stirewalt M (1952) An efficient method for exposure of mice to cercariae of *Schistosoma mansoni*. *The Journal of parasitology* 38: 19-23.
30. Pellegrino J, Oliveira CA, Faria J, Cunha AS (1962) New approach to the screening of drugs in experimental schistosomiasis mansoni in mice. *The American journal of tropical medicine and hygiene* 11: 201.
31. Urayama S, Zou W, Brooks K, Tolstikov V (2010) Comprehensive mass spectrometry based metabolic profiling of blood plasma reveals potent

- discriminatory classifiers of pancreatic cancer. Rapid Communications in Mass Spectrometry 24: 613-620.
32. Bligh E, Dyer WJ (1959) A rapid method of total lipid extraction and purification. Canadian journal of biochemistry and physiology 37: 911-917.
  33. Furlong S (1991) Unique roles for lipids in *Schistosoma mansoni*. Parasitology Today 7: 59-62.
  34. Young BW, Podesta RB (1982) Major phospholipids and phosphatidylcholine synthesis in adult *Schistosoma mansoni*. Molecular and biochemical parasitology 5: 165-172.
  35. Fusco A, Salafsky B, Ellenberger B, Li L-H (1988) *Schistosoma mansoni*: correlations between mouse strain, skin eicosanoid production, and cercarial skin penetration. The Journal of parasitology: 253-261.
  36. Abath FG, Werkhauser RC (1996) The tegument of *Schistosoma mansoni*: functional and immunological features. Parasite immunology 18: 15-20.
  37. McLaren DJ (1984) Disguise as an evasive stratagem of parasitic organisms. Parasitology 88: 597-611.
  38. Fried B, Haseeb MA (1991) Role of lipids in *Schistosoma mansoni*: Parasitol Today. 1991 Aug;7(8):204; author reply 204.
  39. Smith TM, Brooks TJ (1969) Lipid fractions in adult *Schistosoma mansoni*. Parasitology 59: 293-298.
  40. Shaw J, Marshall I, Erasmus D (1977) *Schistosoma mansoni*: In Vitro *Schistosoma mansoni*: Stimulation of vitelline cell development by extracts of male worms. Experimental Parasitology 42: 14-20.
  41. Hockley DJ, McLaren DJ (1973) *Schistosoma mansoni*: Changes in the outer membrane of the tegument during development from cercaria to adult worm. International Journal for Parasitology 3: 13-20.
  42. Brouwers JF, Van Hellemond JJ, van Golde LM, Tielens AG (1998) Ether lipids and their possible physiological function in adult *Schistosoma mansoni*. Molecular and biochemical parasitology 96: 49-58.
  43. Espinoza B, Silman I, Arnon R, Tarrab-Hazdai R (1991) Phosphatidylinositol-specific phospholipase C induces biosynthesis of acetylcholinesterase via diacylglycerol in *Schistosoma mansoni*. European journal of biochemistry 195: 863-870.
  44. Malgat M, Maurice A, Baraud J (1986) Sphingomyelin and ceramide-phosphoethanolamine synthesis by microsomes and plasma membranes from rat liver and brain. Journal of lipid research 27: 251-260.
  45. Testi R (1996) Sphingomyelin breakdown and cell fate. Trends in biochemical sciences 21: 468-471.
  46. Wiest PM, Burnham DC, Olds GR, Bowen WD (1992) Developmental expression of protein kinase C activity in *Schistosoma mansoni*. The American journal of tropical medicine and hygiene 46: 358-365.
  47. Redman CA, Kennington S, Spathopoulou T, Kusel JR (1997) Interconversion of sphingomyelin and ceramide in adult *Schistosoma mansoni*. Molecular and biochemical parasitology 90: 145-153.
  48. Kolesnick R, Golde DW (1994) The sphingomyelin pathway in tumor necrosis factor and interleukin-1 signaling. Cell 77: 325-328.

49. Hannun YA (1994) The sphingomyelin cycle and the second messenger function of ceramide. *Journal of Biological Chemistry-Paper Edition* 269: 3125-3128.
50. Obeid LM, Linardic CM, Karolak LA, Hannun YA (1993) Programmed cell death induced by ceramide. *Science* 259: 1769-1771.
51. Andrieu N, Salvayre R, Levade T (1994) Evidence against involvement of the acid lysosomal sphingomyelinase in the tumor-necrosis-factor-and interleukin-1-induced sphingomyelin cycle and cell proliferation in human fibroblasts. *Biochem J* 303: 341-345.
52. Belka C, Wiegmann K, Adam D, Holland R, Neuloh M, et al. (1995) Tumor necrosis factor (TNF)-alpha activates c-raf-1 kinase via the p55 TNF receptor engaging neutral sphingomyelinase. *The EMBO journal* 14: 1156.
53. Raines M, Kolesnick R, Golde D (1993) Sphingomyelinase and ceramide activate mitogen-activated protein kinase in myeloid HL-60 cells. *Journal of Biological Chemistry* 268: 14572-14575.
54. Amiri P, Locksley RM, Parslow TG, Sadick M, Rector E, et al. (1992) Tumour necrosis factor  $\alpha$  restores granulomas and induces parasite egg-laying in schistosome-infected SCID mice.
55. Garside P, Sands WA, Kusel JR, Hagan P (1996) Is the induction of apoptosis the mechanism of the protective effects of TNF $\alpha$  in helminth infection? *Parasite immunology* 18: 111-113.
56. Hagan P, Garside P, Kusel J (1993) Is tumour necrosis factor alpha the molecular basis of concomitant immunity in schistosomiasis? *Parasite immunology* 15: 553-557.
57. Pinlaor S, Prakobwong S, Boonmars T, Wongkham C, Pinlaor P, et al. (2009) Effect of praziquantel treatment on the expression of matrix metalloproteinases in relation to tissue resorption during fibrosis in hamsters with acute and chronic *< i>Opisthorchis viverrini</i>* infection. *Acta tropica* 111: 181-191.
58. Cunha V, Noël F (1997) Praziquantel has no direct effect on (Na $^{+}$ +K $^{+}$ )-ATPases and (Ca $^{2+}$ -Mg $^{2+}$ ) ATPases of *< i>Schistosoma mansoni</i>*. *Life sciences* 60: PL289-PL294.
59. You H, McManus DP, Hu W, Smout MJ, Brindley PJ, et al. (2013) Transcriptional responses of *in vivo* praziquantel exposure in schistosomes identifies a functional role for calcium signalling pathway member CamKII. *PLoS pathogens* 9: e1003254.

## **CAPÍTULO III**

**Analisando o ciclo de vida do *Schistosoma*  
*mansonii* utilizando Espectrometria de Massas  
de Alta-Resolução.**

# **Screening the life cycle of *Schistosoma mansoni* using High-Resolution Mass Spectrometry**

**Mônica Siqueira Ferreira<sup>1</sup>, Diogo Noin de Oliveira<sup>1</sup>, Rosimeire Nunes de Oliveira<sup>2</sup>, Silmara Marques Allegretti<sup>2</sup>, Rodrigo Ramos Catharino<sup>1\*</sup>**

**1** Innovare Biomarkers Laboratory, Medicine and Experimental Surgery Nucleus, University of Campinas, 13083-877, Campinas, São Paulo, Brazil

**2** Biology Institute, Animal Biology Department, University of Campinas, 13083-877, Campinas, São Paulo, Brazil.

**\*Corresponding author:** Dr. Rodrigo Ramos Catharino. Medicine and Experimental Surgery Department, School of Medical Sciences, University of Campinas. Rua Cinco de Junho, 350 – Cidade Universitária, Campinas, São Paulo, Brazil, 13083-877. Tel.: +55 (19) 3521-9138. E-mail: rrc@fcm.unicamp.br

## **Abstract**

Schistosomiasis is a common tropical disease caused by *Schistosoma* sp. Schistosomiasis' pathogenesis is known to vary according to the worms' strain. Moreover, high parasitical virulence is directly related to eggs release and granulomatous inflammation in the host's organs. This virulence might be influenced by different classes of molecules, such as lipids. Therefore, better understanding the metabolic profile of these organisms is necessary, especially for an increased potential of unraveling strain virulence mechanisms and resistance to existing treatments. In this report, direct-infusion electrospray high-resolution mass spectrometry (ESI(+)-HRMS) along with the lipidomic platform were employed to rapidly characterize and differentiate two Brazilian *Schistosoma mansoni* strains (BH and SE) in three stages of their life cycle: eggs, miracidia and cercariae, with samples from experimental animals (Swiss/SPF mice). Furthermore, urine samples of the infected and uninfected mice were analyzed to assess the possibility of direct diagnosis. All samples were differentiated using multivariate data analysis, PCA, which helped electing markers from distinct lipid classes; phospholipids, diacylglycerols and triacylglycerols, for example, clearly presented different intensities in some stages and strains, as well as in urine samples. This indicates that biochemical characterization of *S. mansoni* may help narrowing-down the investigation of new therapeutic targets according to strain composition and

aggressiveness of disease. Interestingly, lipid profile of infected mice urine varies when compared to control samples, indicating that direct diagnosis of schistosomiasis from urine may be feasible.

**Keywords:** *Schistosoma mansoni*; HR-FTMS; lipid profile; life cycle.

**Abbreviations:** ESI, electrospray. HR-FTMS, high-resolution Fourier transform mass spectrometry; TLC, thin-layer chromatography; GC-MS, gas chromatography coupled with mass spectrometry; HPLC, high performance liquid chromatography; MALDI-MS, matrix-assisted laser desorption/ionization mass spectrometry; MSI, mass spectrometry imaging; ESI-MS, Electrospray Mass Spectrometry; PCA, Principal Component Analysis; TG, triacylglycerol; DG, diacylglycerol; PKC, protein kinase C; PI, phosphatidylinositol; PS, phosphatidylserine; GSL, glycosphingolipids; Glc-Cer, glucosylceramides; Gal-Cer, galactosylceramides; DA, dodecanoic acid.

## 1. Introduction

Schistosomiasis is a tropical disease caused by a trematode of the genus *Schistosoma* [1]. Between five *Schistosoma* species, the main disease-causing species are *Schistosoma mansoni*, *S. japonicum* and *S. haematobium*; among these, *S. mansoni* is the most prominent and important one, not only for its wide global distribution, but also for its public health and social importance, especially in developing countries [2-5].

The parasite's life cycle is already well described: transmission happens when skin is in contact with fresh water infested with the intermediate hosts, *Biomphalaria sp.* snails, infected with cercariae. After cercarial penetration through mammalian skin, it loses its tail and transform into schistosomula, which resides in the skin for up to 72 hours before entering a blood vessel. After a lung passage, the parasites migrate to the portal venous system, where they mature as male and female worms and deposit hundreds of eggs daily. These eggs reach the gut, and are then eliminated through the feces. When in contact with fresh water, eggs release miracidia, which infect *Biomphalaria sp.* snails. Within the snail, the asexual form multiplies in order to develop the cercariae, restarting the cycle [1, 6]. Apart from the concerns surrounding schistosomiasis itself, numerous works have stated that there may be a close relationship between this disease and the development of cancer [7-9]

It has been suggested that different strains present distinct characteristics in pre-patent period, such as pathogenicity, response to treatments and morphological differences between the adult worms [10]. Yoshioka, Zanotti-Magalhães, Magalhães and Linhares [11] compared the pathogenesis of three

strains of *Schistosoma* from different geographical regions in Brazil: SR (Santa Rosa, Campinas, SP), BH (Belo Horizonte, MG) and SJ (São José dos Campos, SP). Obtained data have demonstrated that SR strain presents lower pathogenicity than the other two. This has been inferred due to its decreased yield of worms and shed eggs, lower number and size of granulomas in the liver and intestine.

Schistosomes have been characterized using analytical approaches based on extraction methodologies, such as TLC, GC-MS and HPLC [12, 13]. Others have also employed MALDI-MS as the main analytical tool [14]. A variation of this technique, MSI, contains an imaging tool, and it was developed to identify the spatial distribution of compounds in any physical sample, such as tissue sections [15], drug tablets [16], cosmetic products [17, 18] and single cells [19]. A recent study in our laboratory demonstrates the lipid composition differences between two strains of *S. mansoni*: SE (Ilha das Flores, SE) and BH [17]. In that work, we analyzed only adult worms using MALDI-MSI and metabolomic tools. Phospholipids, diacylglycerols and triacylglycerols were located in specific structures of the worms' bodies, such as tegument, suckers, reproductive and digestive systems. Furthermore, lipid profiles were found to be different both between strains and males or females.

From the moment of cercarial invasion in mammalian skin to the production of eggs by the adult worm, *S. mansoni* exploits lipid pathways [20]. After host penetration, lipids are important for both maturing and developing the worm [21]. Additionally, lipid content varies according to the different developmental stages of the parasite [22]. Despite these previous studies in *S. mansoni* composition and others of lipid characterization [13, 14], there is still little information about each

stage of schistosomes life cycle, principally comparing two different strains. Based on this, the goal of the present work was to employ lipidomics to characterize and differentiate two *S. mansoni* strains – BH and SE – in three stages of the helminth: eggs, miracidia and cercariae, using Swiss/SPF mice as the definitive biological host. This report describes that it is possible to distinguish two biologically different *S. mansoni* strains at any stage of their life cycles by analyzing their characteristic lipid profile using, as the main analytical tool, direct-infusion ESI-high-resolution mass spectrometry of lipid extracts from each individual stage, along with principal component analysis, based on a previously described approach [23].

High-resolution MS is now being widely utilized as the primary choice for the analysis of complex matrices; this is mostly due to the simplicity of data analysis, since mass accuracy can effectively be used as an adequate parameter, for example in characterization of crude oil [24], and even for accurate identification of lipids from biological samples [25, 26]. By employing MS instruments of resolutions as low as 30,000, combined with the known biological routes, it is possible therefore to provide data accurate enough to be used for chemical characterization of compounds [27].

For our work, we firmly believe that the new information provided will assist future research by linking novel structural data with their probable biological roles, in a powerful combination, that can result in new potential therapeutic targets in the development of antischistosomal drugs.

## **2. Materials and Methods**

All reagents and solvents utilized in the experimental parts were of HPLC grade; reagents were purchased from Sigma-Aldrich (St. Louis, MO, USA) and solvents from J. T. Baker (Xalostoc, Mexico), unless stated otherwise.

### *2.1. Animals and parasite maintenance*

*Schistosoma mansoni* (BH) strain - from Belo Horizonte, MG, Brazil - and (SE) strain - from Ilha das Flores, SE, Brazil were used throughout this study. The strains were hosted in *Biomphalaria glabrata* freshwater snails as intermediates for the parasite early life cycle. This stage was performed under strictly controlled conditions at the Department of Animal Biology, Biology Institute, University of Campinas (UNICAMP), so that not any cross-contamination between strains could happen. Swiss/SPF female mice, weighing  $20\pm5$  g and 4 weeks of age ( $n=10$ ) were used as the definitive hosts. The animals were divided in two distinct groups ( $n=5$ /group), and were briefly exposed to an aqueous suspension containing 100 cercariae of *S. mansoni* of either the BH or the SE strain. Invasion was allowed to proceed by the tail immersion technique [28]. After infection, the mice were maintained under controlled environment (temperature between  $20^{\circ}\text{C}$  and  $22^{\circ}\text{C}$ ) with daylight cycle for 60 days. These experiments were in accordance and approved by the Ethics Commission for the Use of Animals (CEUA/ UNICAMP, protocol No. 2170-1).

## ***2.2. S. mansoni eggs and miracidia obtainment***

8 weeks after infection, mice's feces were separately collected and macerated with dechlorinated water. Sequentially, feces were sieved twice in a mesh of 100 µm followed by 400 µm. The content obtained was placed in a sedimentation calyx. After sedimentation, one part was destined to egg recovery using a glass pipette. The other part of the sediment was incubated at 28°C and exposed to light during one hour for miracidia outbreak. Both eggs and miracidia were stored in microtubes with H<sub>2</sub>O milliQ.

## ***2.3. S. mansoni cercariae obtainment***

Cercariae were obtained according to the protocol proposed by Pellegrino and Katz [29]. For cercariae elimination, *B. glabrata* snails, after 45 days of infection by *S. mansoni*, were put in a snap-cap bottle with dechlorinated water, exposed to light and the temperature of 28°C for two hours. Cercariae were then stored in microtubes with H<sub>2</sub>O milliQ.

## ***2.4. Mice urine obtainment***

To verify possible metabolic changes in infected animals with *S. mansoni*, urine of three groups (n=15/group) of mice was collected: (i) mice with 8 weeks of infection by *S. mansoni* SE strain, (ii) mice with 8 weeks of infection by *S. mansoni* BH strain, and (iii) mice without infection (control group). All animals were isolated without water and food to 40 minutes and 1 mL of urine was collected.

## *2.5. High-resolution Electrospray Mass Spectrometry (ESI-MS) analysis*

Each sample of cercariae, eggs and miracidia of *S. mansoni* was rapidly homogenized in 50 µL of cold chloroform (4 °C). Lipids were extracted adding 100 µL methanol and 40 µL of H<sub>2</sub>O milliQ, according to an adapted Bligh and Dyer [30] protocol. The lower chloroform layer was dried under a stream of nitrogen and dissolved in 50 µL of 1:1 acetonitrile:H<sub>2</sub>O milliQ. To accurately identify chemical markers, all samples were analyzed by high-resolution ESI-MS. For this, a volume of 10 µL urine and lipid extracts were diluted in MeOH (990 µL) (Sigma Aldrich Corporation, St. Louis, USA). Then, these mixtures were filtered with filter 0.22 µm (Merck, Darmstadt, Germany) and formic acid was added to a concentration of 0.1% on each sample. For spectra acquisition, samples were directly infused in an ESI-LTQ-XL Orbitrap Discovery instrument (Thermo Scientific, Bremen, Germany) with nominal resolution of 30,000 (FWHM). All analyses were performed in the positive ion mode with following conditions: sheath gas at 5 arbitrary units, flow rate of 10 µL/min, spray voltage of 5 kV and capillary temperature of 280°C. Spectra were acquired over 60 seconds at the m/z range of 600-1000 for all samples.

## *2.6. Statistical analysis and chemical markers identification*

PCA was performed using Unscrambler v.9.7 (CAMO Software, Trondheim, Norway). The software has clustered samples according to the relationship between m/z and intensity, with the results expressed as groups of samples with the same characteristics when considered these parameters. Mass range was established between m/z 600-1000 and a signal-to-noise threshold in a 3:1 ratio

was established after extracting spectral data in tables of mass x intensity. No normalization was required, since all the samples were acquired within the same parameters. Lipid MAPS online database (University of California, San Diego, CA – [www.lipidmaps.org](http://www.lipidmaps.org)) and METLIN (Scripps Center for Metabolomics, La Jolla, CA) were consulted to help guiding the choice for potential lipid markers. Structural propositions were performed using high resolution as the main parameter. Mass accuracy was calculated and expressed in terms of ppm shifts [31].

### 3. Results

#### 3.1. *Metabolic fingerprint*

Cercariae, miracidia and eggs of two different strains – BH and SE – were subjected to HR-FTMS analysis, as described in methods. Despite similar spectra pattern, multivariate data analysis, namely PCA, made it possible to see the results precisely and clearly enough to elect specific chemical markers that could differentiate each group on each pair comparison (Figures 13-15, A and B; Figure 16A-16C).

#### 3.2. *Statistical analysis and chemical markers identification*

Statistical analysis was performed by comparing SE and BH strains in different stages of *S. mansoni* life cycle. A previous measurement was performed with all the samples (eggs, miracidia and cercariae) within the two strains (i.e., all samples for BH and all samples for SE, separately). Since that has presented

differentiation, we performed a general PCA contemplating all the samples from both strains, with results presented in Figure 17 (supplementary material). For assertive compound characterization purposes, the considered lipid markers were the ones obtained in the separate PCAs. As shown in Figure 13C, 14C, 15C and 16C, all groups were clearly separated with accuracy higher than 85%.

For the characterization of lipid markers, experimental *m/z* ratios obtained by HR-FTMS were compared to the theoretical data, using the exact theoretical mass as the main parameter. The structures were also taken from METLIN database to obtain an ID number that will help promptly identify these molecules in future experiments. Table 1 organizes this dataset as: the identified lipid species in each sample group (precursor ion) and the mass errors (difference between the observed and theoretical masses) for each signal observed in high resolution, measured in ppm; all measurements have presented a deviation lower than 2 ppm.

*Figure 13. Representative fingerprinting spectra and PCA of *S. mansoni* eggs. Both spectra were acquired in positive ion mode by HR-FTMS. (A) Spectrum of eggs SE strain. (B) Spectrum of eggs BH strain. (C) PCA loadings, demonstrating the two distinct groups ( $n=5$ /group). The explained variances (X-expl) are shown on inferior part of the figure. ■, eggs SE strain. ●, eggs BH strain.*

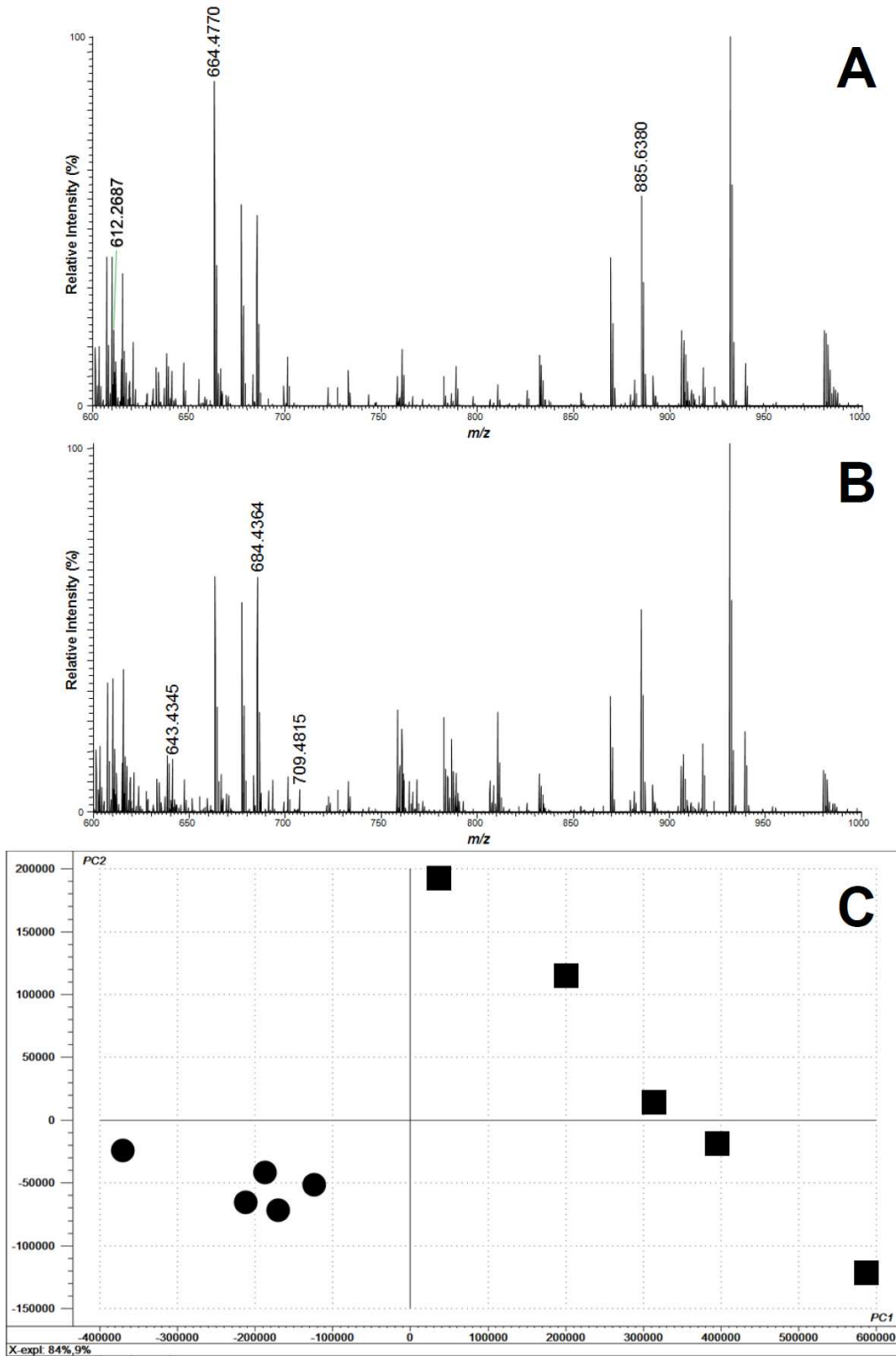


*Figure 14. Representative fingerprinting spectra and PCA of S. mansoni miracidia. Both spectra were acquired in positive ion mode by HR-FTMS. (A) Spectrum of miracidia SE strain. (B) Spectrum of miracidia BH strain. (C) PCA loadings, demonstrating the two distinct groups ( $n=5$ /group). The explained variances ( $X\text{-expl}$ ) are shown on inferior part of the figure. ■, miracidia SE strain. ●, miracidia BH strain.*

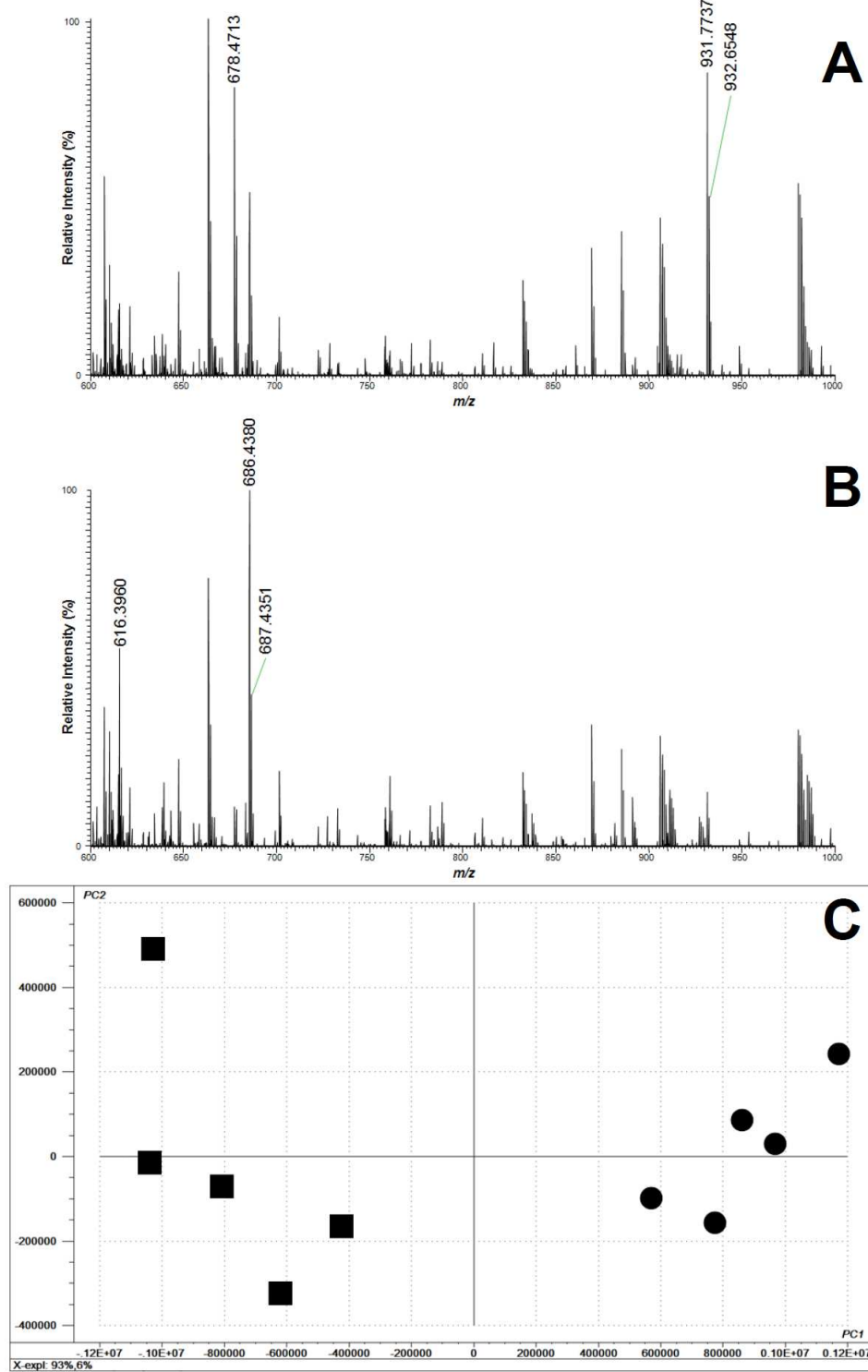


**Figure 15.** Representative fingerprinting spectra and PCA of *S. mansoni* cercariae. Both spectra were acquired in positive ion mode by HR-FTMS. (A) Spectrum of cercariae SE strain. (B) Spectrum of cercariae BH strain. (C) PCA loadings, demonstrating the two distinct groups ( $n=5$ /group). The explained variances ( $X\text{-expl}$ ) are shown on inferior part of the figure. ■, cercariae SE strain. ●, cercariae BH strain.

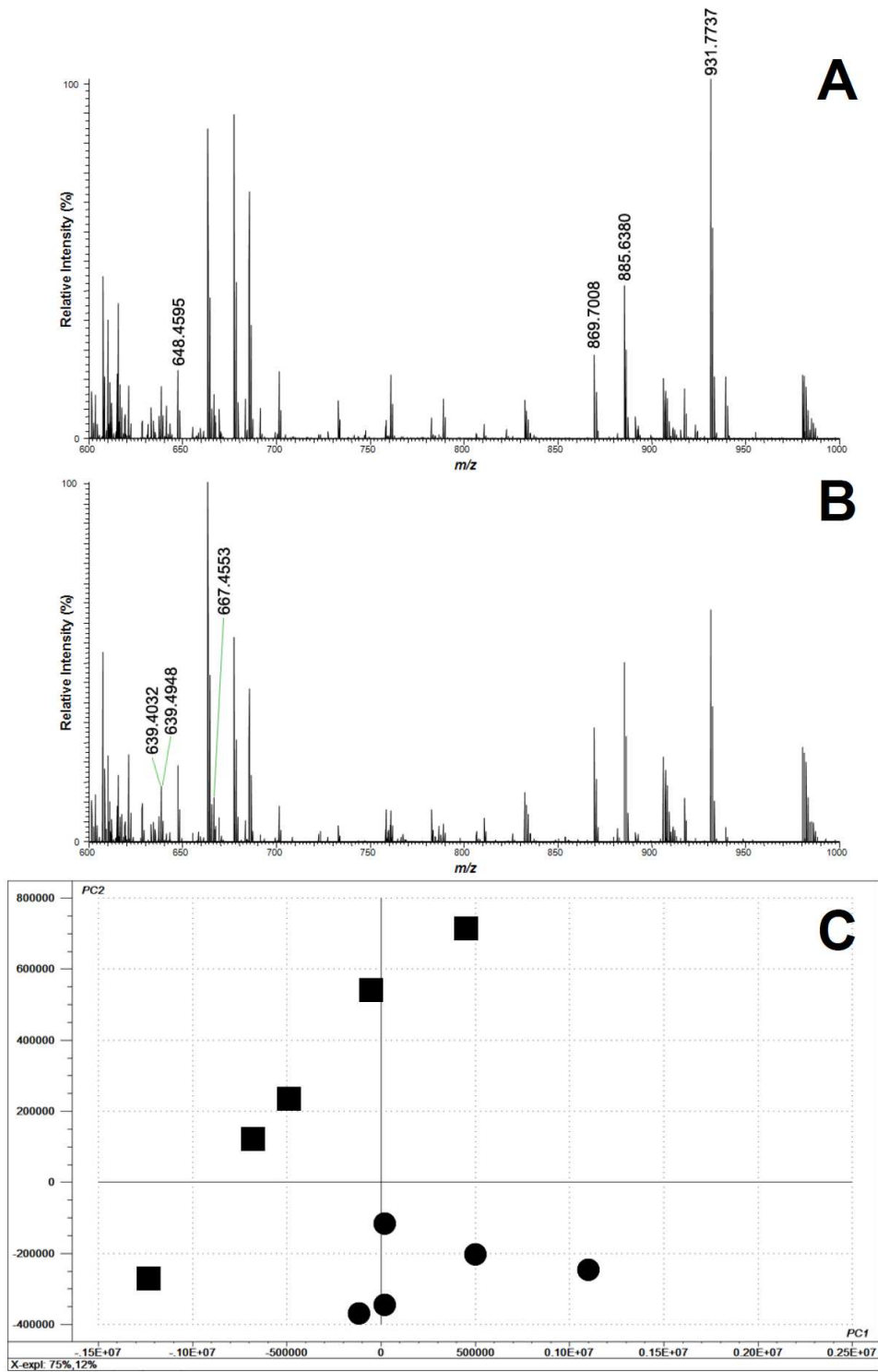


**Figure 16.** Representative fingerprinting spectra and PCA of urine of mice infected or not by *S. mansoni*. All spectra were acquired in positive ion mode by HR-FTMS. (A) Spectrum of urine of mice infected by SE strain. (B) Spectrum of urine of mice infected by BH strain. (C) Spectrum of urine of control mice. (D) PCA loadings, demonstrating the three distinct groups ( $n=15$ /group). The explained variances ( $X_{\text{expl}}$ ) are shown on inferior part of the figure. ■, SE strain. ●, BH strain. ▲, control group.

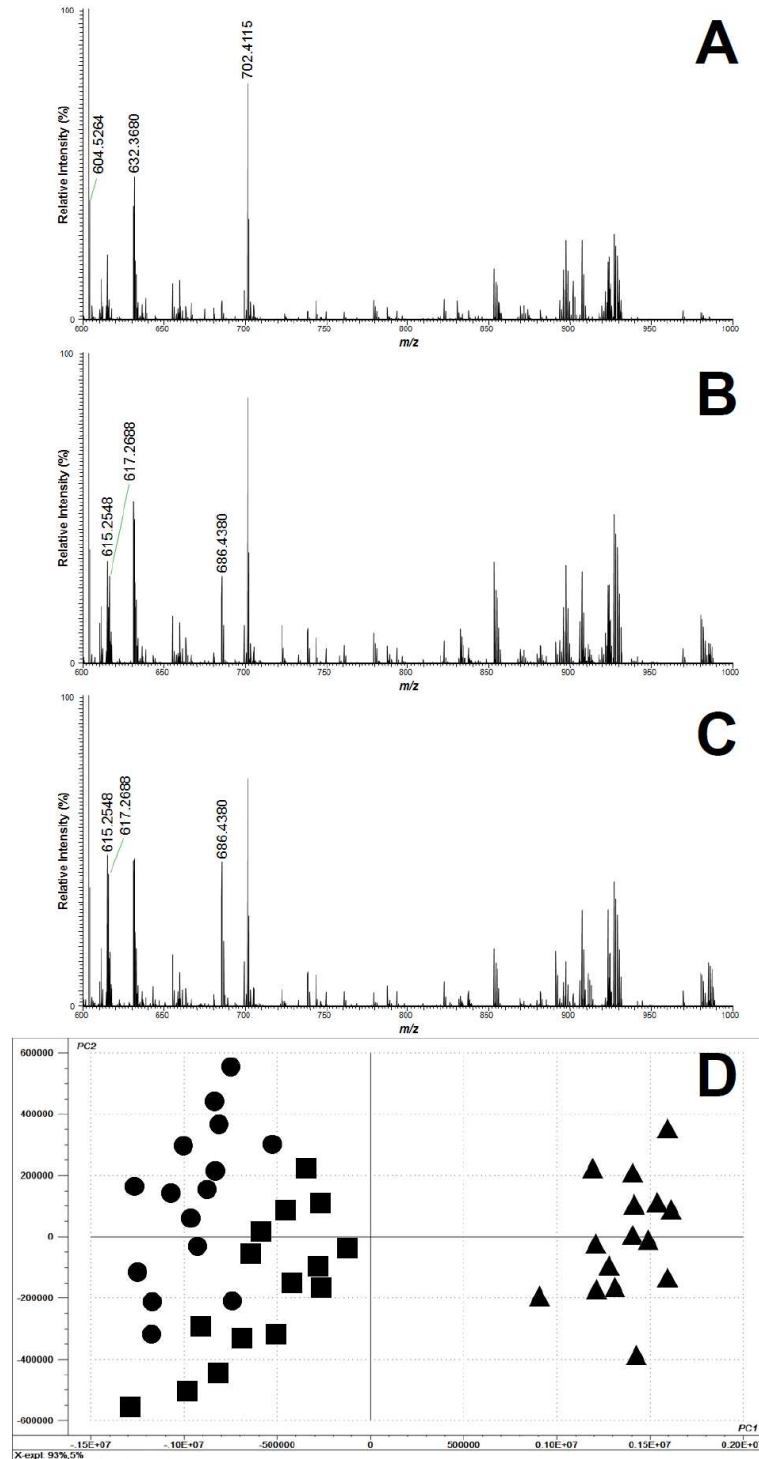


*Figure 17. PCA plot showing the differentiation between BH and SE eggs, cercariae and miracidia of *S. mansoni*.*

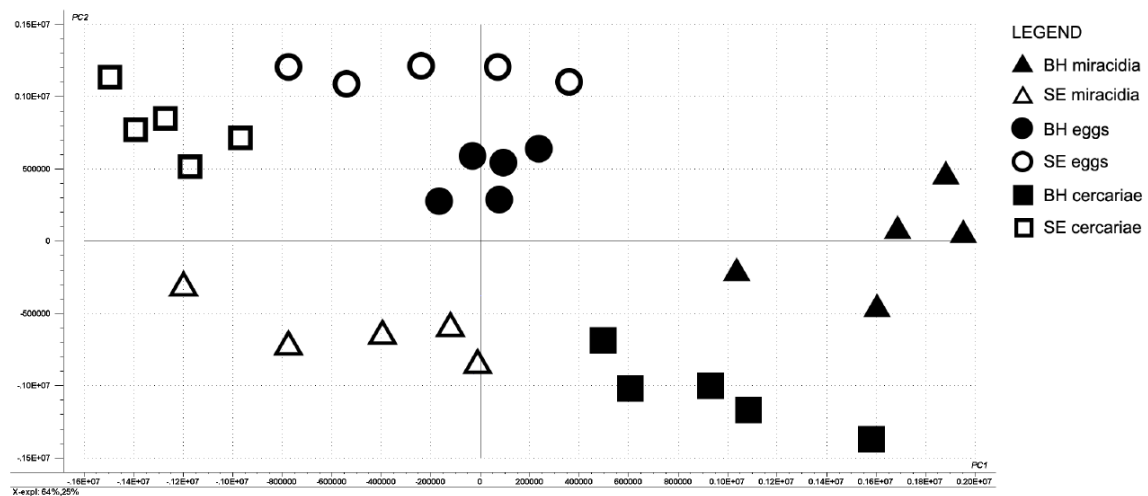


*Table 3. Lipid chemical markers identified via HR-FTMS of S. mansoni eggs, miracidia and cercariae; and mice's urine infected or not by S. mansoni (positive ion mode). Identification is based on the comparison between the exact and theoretical masses of each compound and Lipid Maps and METLIN databases.*

Sample	Molecule	Experimental mass ( <i>m/z</i> )	Theoretical Mass ( <i>m/z</i> )	Error (ppm)	LM ID*	MID**
Urine SE/BH	[PI(18:4/0:0)+Na] <sup>+</sup>	615.2548	615.2541	1,14	LMGP06050017	81182
	[PI(18:3/0:0)+Na] <sup>+</sup>	617.2688	617.2697	-1,46	LMGP06050016	81181
	[PS(16:0/12:0)+Na] <sup>+</sup>	686.4380	686.4367	1,89	LMGP03030001	78741
Urine CT	[Cer(16:1/20:0)+Na] <sup>+</sup>	604.5264	604.5275	-1,82	LMSP02010084	102987
	[PI(17:2/0:0)+Na] <sup>+</sup>	605.2688	605.2697	-1,49	LMGP06050015	81180
	[PE(12:0/13:0)+K] <sup>+</sup>	632.3680	632.3688	-1,27	LMGP02010008	3868
	[PS(16:0/12:0)+K] <sup>+</sup>	702.4115	702.4107	1,14	LMGP03030001	78741
Eggs SE	[PS(22:4/0:0)+K] <sup>+</sup>	612.2687	612.2698	-1,80	LMGP03050014	78841
	[GlcCer(14:2/16:0)+Na] <sup>+</sup>	664.4770	664.4759	1,66	LMSP0501AA52	103292
	[TG(15:1/17:2/20:5)+K] <sup>+</sup>	885.6380	885.6369	1,24	LMGL03015467	101315
Eggs BH	[PA(12:0/20:3)+H] <sup>+</sup>	643.4345	643.4333	1,86	LMGP10010059	81225
	[PE(16:0/14:1)+K] <sup>+</sup>	684.4364	684.4365	-0,15	LMGP02030010	77588
	[DG(20:5/22:6/0:0)+Na] <sup>+</sup>	709.4815	709.4802	1,83	LMGL02010286	4660
	[PS(19:1/22:0)+Na] <sup>+</sup>	882.6183	882.6195	-1,36	LMGP03010506	78170
Cercaria SE	[PE(15:1/14:0)+H] <sup>+</sup>	648.4595	648.4599	-0,62	LMGP02010476	76711
	[TG(16:0/17:1/17:1)+K] <sup>+</sup>	869.7008	869.6995	1,49	LMGL03010032	4731
	[TG(15:1/17:2/20:5)+K] <sup>+</sup>	885.6380	885.6369	1,24	LMGL03015467	101315
	[TG(18:2/18:3/20:0)+Na] <sup>+</sup>	931.7737	931.7725	1,29	LMGL03010591	37090
Cercaria BH	[PA(12:0/20:5)+H] <sup>+</sup>	639.4032	639.4020	1,88	LMGP10010061	81227
	[DG(18:2/18:2/0:0)+Na] <sup>+</sup>	639.4948	639.4959	-1,72	LMGL02010063	4371
	[PG(14:0/14:0)+H] <sup>+</sup>	667.4553	667.4544	1,35	LMGP04010009	40840
Miracidium SE	[PI-Cer(18:0/24:0)+Na] <sup>+</sup>	932.6548	932.6562	-1,50	LMSP03030016	103145
	[TG(18:2/18:3/20:0)+Na] <sup>+</sup>	931.7737	931.7725	1,29	LMGL03010591	37090
	[PS(16:0/13:0)+H] <sup>+</sup>	678.4713	678.4704	1,33	LMGP03030002	78742
Miracidium BH	[DA(12:0/12:0)+Na] <sup>+</sup>	616.3960	616.3949	1,78	LMGP02010341	40737
	[PS(16:0/12:0)+Na] <sup>+</sup>	686.4380	686.4367	1,89	LMGP03030001	78741
	[PA(17:0/15:0)+K] <sup>+</sup>	687.4351	687.4362	-1,60	LMGP10010897	82063

SE, SE strain. BH, BH strain. CT, control sample. PI, Phosphoinositol. PS, Phosphatidylserine. Cer, Ceramide. PE, Phosphoethanolamine. GlcCer, Glucosylceramide. TG, Triacylglycerol. PA, Phosphatidic Acid. DG, Diacylglycerol. DA, Dodecanoic Acid. ppm, part per million.

\*LMID, Lipid Maps ID. \*\*MID, METLIN ID.

#### **4. Discussion**

Previous studies have demonstrated that distinct *S. mansoni* strains presented different lipid composition [10, 11]. It was also demonstrated that lipid markers can be assigned to specific regions in adult worms [17]. Furthermore, lipid composition may vary according to the developmental stages of the parasite [22]. Based on this, we performed several analyses to characterize and differentiate three stages of *S. mansoni*, as well as the urine of mice, infected or not. Our results evidenced clear segregation of groups. Generally, phospholipids and triacylglycerols represent the major classes, as also demonstrated by Brouwers, Smeenk, van Golde and Tielens [32].

TGs were present in SE strain, in all three analyzed stages, and all identified species presented on Table 1 were pointed as group markers by PCA. Although the biochemical function of TG in *S. mansoni* is unclear, it is unlikely to be linked to energy production, since ATP cannot be generated through the  $\beta$ -oxidation of fatty acids in these organisms [33]. For that reason, there is a hypothesis that TG synthesis in schistosomes is used to prevent high intracellular free fatty acid concentrations [32]. Because these stages of *S. mansoni* SE strain were reported for the first time, studies focused on functional and/or molecular biology will be required to understand the function of this lipid group.

Diacylglycerols were presented as group-markers for the BH strain, specifically in eggs and cercariae. This result is in accordance to Wiest, Kunz and Miller [34], that described the protein kinase C (PKC) activity during *S. mansoni* maturation, cercariae to adult worms. PKC regulates many cellular functions in

eukaryotic cells, such as differentiation, cell growth, and metabolism [35-37]. In this context, phospholipase C, when activated by extracellular signals, hydrolyses phosphatidylinositol, which in turn results in the formation of following intracellular second messengers: inositol 1, 4, 5-trisphosphate and DGs. The first mobilizes  $\text{Ca}^{+2}$  from intracellular stores while PKC is activated by diacylglycerol to regulate intracellular events [35]. Moreover, phosphatidylserine may also stimulate PKC. Thus, we propose that this way can be greatly related to major pathogenicity of BH strain, as described by Yoshioka, Zanotti-Magalhães, Magalhães and Linhares [11]. However, further investigation on clinical and/or functional biology of these molecules is necessary to confirm this hypothesis.

Part of the pathogenicity in schistosomiasis is measured by the number of granulomas in organs, such as gut, liver and lung [11]. These granulomatous inflammations are induced primarily by schistosome egg antigens [38]. Glycoproteins and glycolipids have been identified as egg antigens in *S.mansoni* [38-40]. Among glycolipids, glycosphingolipids were found as the major constituting class in *S.mansoni*'s eggs [41]. According to Khoo, Chatterjee, Caulfield, Morris and Dell [41], the short neutral GSLs in *S.mansoni* probably comprises glucosylceramides and galactosylceramides, supporting the result found in our study, which Glc-Cer is a lipid marker in the eggs of SE strain. Furthermore, there is evidence indicating that GSLs obtained from different life-cycle stages of the *S.mansoni* may potentially modulate the response of human dendritic cells, which play a major role in the regulation of the host's adaptive immunity [42].

Information on the lipid composition of *S.mansoni* miracidia is scarce. In this study, we identified some chemical markers in miracidia of the two strains that

could help to understand the metabolism in this stage of life cycle. One of the compounds is dodecanoic acid, found in BH strain. There are reports of DA facilitating *S. mansoni* cercariae penetration [43]. Miracidium is a free-living motile form and as explained in introduction, the infective form of *Biomphalaria sp.* snails [44]. A hypothesis of DA presence in miracidia is that it could help their penetration in the intermediate host.

With all of the obtained information, that is, being able to differentiate *S. mansoni* life stages by characteristic lipids using high-resolution MS, another focus of our study was to differentiate the urine of mice infected or not by the helminth; PCA results demonstrated that metabolic profiles of infected mice to both strains, BH and SE, are clearly different with respect to control mice. However, regardless of the worm's strain, there is no significant difference between BH or SE in urine, hence, the only result that we were able to obtain is simply whether the animal was infected or not. This comparison is interesting enough and shows the potential of HR-FTMS to enable the rapid diagnosis of schistosomiasis, since there were no metabolic differences between SE and BH strains in urine [45]. For this, monoclonal antibodies are used to detect circulating cathodic antigen and several incubation processes are required. Although the authors demonstrated great sensitivity and specificity, this method is time-consuming [45]. In contrast, mass spectrometry allows rapid and sensitive analysis, with good reproducibility [17].

## 5. Conclusions

We feel our approach was successful in demonstrating and confirming [17] that *S. mansoni* composition depends on strain, and each stage of life cycle had little distinctions of metabolic profile. This distinction could be related to different pathogenesis, as previously described [11, 46]. Our approach shows that HRMS is a very fast and reliable tool for these purposes, since it provides results in a very straightforward way, with an expeditious analytical chain of circa 45 minutes, from sample preparation to final results. Furthermore, characterization of eggs, miracidia and cercariae of *S. mansoni* show great potential to allow schistosomiasis control by investigating new targets according strain composition. Finally, the potential for rapid diagnosis by urine of the mammalian host adds to the literature as a new method to be developed and described in future contributions.

**Acknowledgments:** This work was financially supported by CAPES (Coordination for the Improvement of Higher Level -or Education- Personnel), FAPESP (São Paulo Research Foundation), CNPq and INCT (National Science and Technology Institutes).

## References

- [1] B. Gryseels, K. Polman, J. Clerinx, L. Kestens, *The Lancet*, 368 (2006) 1106.
- [2] S.J. Krauth, J.T. Coulibaly, S. Knopp, M. Traoré, E.K. N'Goran, J. Utzinger, *PLoS neglected tropical diseases*, 6 (2012) e1969.
- [3] T. Handzel, D. Karanja, D.G. Addiss, A.W. Hightower, D.H. Rosen, R. Moyou-Somo, L. Kouemeni, B. Ndjamen, J. Ngogang, R. Dongla, *American Journal of Tropical Medicine and Hygiene*, 69 (2013) 318.
- [4] D.M. Barboza, C. Zhang, N.C. Santos, M. Matos, B.L. Silva, C.V.V. Rollemburg, F.J.R. de Amorim, M.T. Ueta, C.M. de Melo, J.A.P. de Almeida, *CEP*, 49045 (2012) 100.
- [5] J. Utzinger, G. Raso, S. Brooker, D. De Savigny, M. Tanner, N. Ørnberg, B. Singer, E. N'goran, *Parasitology*, 136 (2009) 1859.
- [6] T. Quack, S. Beckmann, C. Greveling, *Berliner und Munchener tierarztliche Wochenschrift*, 119 (2006) 365.
- [7] C. Ye, S. Tan, L. Jiang, M. Li, P. Sun, L. Shen, H. Luo, *Molecular Medicine Reports*, 8 (2013) 1089.
- [8] O.E. Salim, H. Hamid, S.O. Mekki, S.H. Suleiman, S.Z. Ibrahim, *World J Surg Oncol*, 13 (2010) 68.
- [9] W. Zhang, P.-J. Wang, X. Shen, G.-I. Wang, X.-h. Zhao, S. Seema, S.-q. Zheng, M.-h. Li, *European journal of radiology*, 81 (2012) e835.
- [10] E.M. Martinez, R.H. Neves, R.M.F.d. Oliveira, J.R. Machado-Silva, L. Rey, *Revista da Sociedade Brasileira de Medicina Tropical*, 36 (2003) 557.
- [11] L. Yoshioka, E.M. Zanotti-Magalhães, L.A. Magalhães, A.X. Linhares, *Revista da Sociedade Brasileira de Medicina Tropical*, 35 (2002) 203.
- [12] B.W. Young, R.B. Podesta, *The Journal of parasitology*, 72 (1986) 802.
- [13] M. Wuhrer, R.D. Dennis, M.J. Doenhoff, G. Lochnit, R. Geyer, *Glycobiology*, 10 (2000) 89.
- [14] S. Frank, I. van Die, R. Geyer, *Glycobiology*, 22 (2012) 676.
- [15] E.G. Solon, (2007).
- [16] L.R. Rodrigues, D.N.d. Oliveira, M.S. Ferreira, R.R. Catharino, *Analytica Chimica Acta*, In Press (2014).
- [17] M.S. Ferreira, D.N. de Oliveira, R.N. de Oliveira, S.M. Allegretti, A.E. Vercesi, R.R. Catharino, *Journal of Mass Spectrometry*, 49 (2014) 86.
- [18] D.N. de Oliveira, M. Siqueira, S. Sartor, R. Catharino, *International Journal of Cosmetic Science*, 35 (2013) 467.
- [19] M.S. Ferreira, D.N. de Oliveira, R.F. Gonçalves, R.R. Catharino, *Analytica Chimica Acta* (2013).
- [20] S.T. Furlong, *Parasitol Today*, 7 (1991) 59.
- [21] P. Nirde, M.L. De Reggi, G. Tsoupras, G. Torpier, P. Fressancourt, A. Capron, *FEBS Lett*, 168 (1984) 235.
- [22] S.T. Furlong, J.P. Caulfield, *Exp Parasitol*, 65 (1988) 222.
- [23] D. Schwudke, J.T. Hannich, V. Surendranath, V. Grimard, T. Moehring, L. Burton, T. Kurzchalia, A. Shevchenko, *Analytical Chemistry*, 79 (2007) 4083.

- [24] P.A. Eckert, P.J. Roach, A. Laskin, J. Laskin, *Analytical Chemistry*, 84 (2011) 1517.
- [25] N.E. Manicke, A.L. Dill, D.R. Ifa, R.G. Cooks, *Journal of Mass Spectrometry*, 45 (2010) 223.
- [26] S.-P. Hui, T. Sakurai, F. Ohkawa, H. Furumaki, S. Jin, H. Fuda, S. Takeda, T. Kurosawa, H. Chiba, *Anal Bioanal Chem*, 404 (2012) 101.
- [27] L.S. Eberlin, C.R. Ferreira, A.L. Dill, D.R. Ifa, R.G. Cooks, *Biochimica et Biophysica Acta (BBA) - Molecular and Cell Biology of Lipids*, 1811 (2011) 946.
- [28] L. Olivier, M.A. Stirewalt, *J Parasitol*, 38 (1952) 19.
- [29] J. Pellegrino, N. Katz, *Adv Parasitol*, 6 (1968) 233.
- [30] E.G. Bligh, W.J. Dyer, *Canadian journal of biochemistry and physiology*, 37 (1959) 911.
- [31] J.C. Erve, W. DeMaio, R.E. Talaat, *Rapid Communications in Mass Spectrometry*, 22 (2008) 3015.
- [32] J.F. Brouwers, I. Smeenk, L.M. van Golde, A.G. Tielens, *Molecular and biochemical parasitology*, 88 (1997) 175.
- [33] J. Barrett, *Biochemistry of parasitic helminths*, MacMillan Publishers Ltd., 1981.
- [34] P. Wiest, S. Kunz, K. Miller, *PARASITOLOGY-CAMBRIDGE-*, 109 (1994) 461.
- [35] U. Kikkawa, Y. Nishizuka, *Annual review of cell biology*, 2 (1986) 149.
- [36] Y. Nishizuka, (1984).
- [37] Y. Nishizuka, *Nature*, 334 (1988) 661.
- [38] D.L. Boros, K.S. Warren, *The Journal of experimental medicine*, 132 (1970) 488.
- [39] C.E. Carter, D.G. Colley, *The Journal of Immunology*, 122 (1979) 2204.
- [40] J. Weiss, J. Magnani, M. Strand, *The Journal of Immunology*, 136 (1986) 4275.
- [41] K.-H. Khoo, D. Chatterjee, J.P. Caulfield, H.R. Morris, A. Dell, *Glycobiology*, 7 (1997) 653.
- [42] I. van Die, C.M. van Stijn, H. Geyer, R. Geyer, *Methods in enzymology*, 480 (2010) 117.
- [43] W. Haas, R. Schmitt, *Zeitschrift für Parasitenkunde*, 66 (1982) 293.
- [44] A.J. MacInnis, *The Journal of parasitology* (1965) 731.
- [45] L. Van Etten, C.C. Folman, T.A. Eggelte, P.G. Kremsner, A.M. Deelder, *Journal of clinical microbiology*, 32 (1994) 2404.
- [46] K.S. Warren, *Transactions of the Royal Society of Tropical Medicine and Hygiene*, 61 (1967) 795.

## **CONCLUSÕES GERAIS**

A metodologia proposta por este trabalho, denominada Parasitômica, apresenta-se como uma nova alternativa para o estudo de parasitas, podendo ser utilizada como ferramenta complementar no controle de doenças negligenciadas, como a esquistossomose. Inicialmente, a caracterização e diferenciação dos vermes adultos de diferentes cepas *S. mansoni* foi o foco principal, com o objetivo de auxiliar no entendimento dos diferentes níveis de virulência de uma mesma espécie. Em sequência, a caracterização das alterações químicas ocorridas no verme adulto exposto ao PZQ permitiu visualizar os diferentes alvos, internos e externos, com maiores modificações químicas causadas pelo fármaco. Tal informação poderá auxiliar tanto na compreensão de vias envolvidas nesse processo, como no desenvolvimento de novos fármacos alternativos que, potencialmente, podem controlar a esquistossomose. Similarmente ao verme adulto, o estudo de caracterização dos componentes do ciclo de *S. mansoni* demonstrou diferença nítida na composição molecular de ambas as cepas, BH e SE. Tal resultado poderá igualmente auxiliar no desenvolvimento de novos alvos terapêuticos. Finalmente, resultados obtidos na análise da urina apontam para um potencial método de diagnóstico de esquistossomose, mais rápido e direto que o convencional. No entanto, mais experimentos são necessários para comprovar essa hipótese, como validação, comparação com outras helmintíases e análises de urina humana.

Dentro desse escopo, considera-se que o trabalho desenvolvido até o momento da apresentação dessa dissertação cumpriu seus objetivos primários de criação de uma nova plataforma analítica voltada para parasitas, bem como sua aplicação em diferentes estágios de desenvolvimento do *S. mansoni*.

## **PERSPECTIVAS FUTURAS**

Devido aos diferentes níveis de virulência e resistência do verme ao fármaco PZQ, diversos estudos têm sido realizados em busca de fármacos alternativos para controle da doença. No entanto, pouco é conhecido da composição química específica de cada cepa. A plataforma Parasitômica possui grande importância para essa caracterização, podendo inclusive localizar as estruturas alvo desses novos fármacos no parasita.

Nesse contexto, estudos relacionados a um fármaco alternativo já estão em vias de análise, juntamente com o Departamento de Parasitologia da Universidade de Campinas. Nesse projeto estão também envolvidos dois alunos de Doutorado. Como até o momento da apresentação desta dissertação não havia resultados significativos, os mesmos não foram incluídos.